PREPARATION AND CHARACTERIZATION OF POLYMERIC BLEND
AND MIXED MATRIX MEMBRANES BY WATER VAPOR INDUCED
PHASE INVERSION

A THESIS SUBMITTED TO
THE GRADUATE SCHOOL OF NATURAL AND APPLIED SCIENCES
OF
MIDDLE EAST TECHNICAL UNIVERSITY

BY

SEREN KİBAR

IN PARTIAL FULFILLMENT OF THE REQUIREMENTS
FOR
THE DEGREE OF MASTER OF SCIENCE
IN
CHEMICAL ENGINEERING

AUGUST 2019

Approval of the thesis:

PREPARATION AND CHARACTERIZATION OF POLYMERIC BLEND AND MIXED MATRIX MEMBRANES BY WATER VAPOR INDUCED PHASE INVERSION

submitted by **SEREN KİBAR** in partial fulfillment of the requirements for the degree of **Master of Science in Chemical Engineering Department, Middle East Technical University** by,

Prof. Dr. Halil Kalıpçılar
Dean, Graduate School of **Natural and Applied Sciences** ⸺⸺⸺⸺

Prof. Dr. Pınar Çalık
Head of Department, **Chemical Engineering** ⸺⸺⸺⸺

Prof. Dr. Halil Kalıpçılar
Supervisor, **Chemical Engineering Dept., METU** ⸺⸺⸺⸺

Examining Committee Members:

Prof. Dr. Levent Yılmaz
Chemical Engineering Dept., METU ⸺⸺⸺⸺

Prof. Dr. Halil Kalıpçılar
Chemical Engineering Dept., METU ⸺⸺⸺⸺

Asst. Prof. Dr. Emre Büküşoğlu,
Chemical Engineering Dept., METU ⸺⸺⸺⸺

Asst. Prof. Dr. Bahar İpek Torun,
Chemical Engineering Dept., METU ⸺⸺⸺⸺

Assoc. Prof. Dr. Berna Topuz
Chemical Engineering Dept., Ankara University ⸺⸺⸺⸺

Date: 29.08.2019

I hereby declare that all information in this document has been obtained and presented in accordance with academic rules and ethical conduct. I also declare that, as required by these rules and conduct, I have fully cited and referenced all material and results that are not original to this work.

Name, Last name: Seren KİBAR

Signature   :

ABSTRACT

PREPARATION AND CHARACTERIZATION OF POLYMERIC BLEND AND MIXED MATRIX MEMBRANES BY WATER VAPOR INDUCED PHASE INVERSION

Kibar, Seren
Master of Science, Department of Chemical Engineering
Supervisor: Prof. Dr. Halil Kalıpçılar

August 2019, 91 pages

Asymmetric polymeric thin film membranes are commonly produced by using non-solvent induced phase inversion process. The membrane solution is cast to a glass plate and then it is brought into contact with a coagulant. Coagulant type affects the asymmetric membrane structure and the skin formation according to phase separation mechanism. They are related with the membrane gas permeation and separation performances.

In this study, asymmetric blend and mixed matrix membranes were produced by using dry/wet phase inversion method. The dry phase inversion were performed by using infrared light, while the wet phase inversion was carried out by using water vapor with 80% relative humidity as non-solvent. To achieve to desired relative humidity value, the membrane casting processes were executed in a conditioning glove box. Polyethersulfone(PES) and polyimide(PI) were used as polymeric materials for blend membrane preparation. Solvents which were used during membrane solution preparation were dimethylformamid(DMF) and tetrahydrofuran(THF). For the mixed matrix membranes, same polymers were used and the 60nm ZIF-8 was used. ZIF-8 has high gas adsorption capacity and has good chemical and thermal stability. Polymeric blend membranes were prepared with the ratio of PES/PI/20/80, PES/PI/50/50 and PES/PI/80/20. The

mixed matrix membranes were produced by adding 10% ZIF-8 filler to the same polymer ratio of blend membranes. H_2, CO_2 and CH_4 permeances of both blend and mixed matrix membranes were measured at 35°C. H_2/CO_2, CO_2/CH_4 and H2/CH4 ideal selectivities were calculated. CO_2/CH_4 mixture separation performances of the membranes were measured by analyzing feed and permeate gas using gas chromatography.

Keywords: polyethersulfone, polyimide, ZIF-8, blend membrane, mixed matrix membrane

ÖZ

SU BUHARI ENDÜKLEME FAZ DEĞİŞİM YÖNTEMİYLE POLİMER HARMANLI VE KARIŞIK MATRİSLİ MEMBRANLARIN ÜRETİLMESİ VE KARAKTERİZASYONU

Kibar, Seren
Yüksek Lisans, Kimya Mühendisliği Bölümü
Tez Danışmanı: Prof. Dr. Halil Kalıpçılar

Ağustos 2019, 91 sayfa

Asimetrik yapıdaki polimerik ince film membranlar genellikle çözücü olmayan faz değişim yöntemi ile üretilirler. Bu yöntemde, membran çözeltisi cam yüzeyin üzerine dökülür ve koagülant ile temas haline getirilir. Koagülant tipi seçimi, faz değişimi mekanizmasına göre asimetrik membran yapısını ve yüzey oluşumunu direkt olarak etkiler ve bu özellikler membran gaz geçirgenliği ve gaz ayırımı performansı ile doğrudan ilgilidir.

Bu çalışmada, asimetrik yapıda polimer harmanlı ve karışık matrisli membranlar kuru/ıslak faz değişimi yöntemi kullanılarak üretildi. Membran üretimi sırasında, ıslak faz değişimi 80% bağıl neme sahip su buharı çözücü olmyan madde olarak kullanarak gerçekleştirilirken, kuru faz değişimi membran yüzeyi kızılötesi ışığa maruz bırakılarak yapıldı. İstenen bağıl nem değerini elde edebilmek için, membran döküm işlemi iklimlendirilmiş ortam kabini içerisinde gerçekleştirildi. Polimer harmanlı membranların hazırlanması için polietersülfon (PES) ve poliimid (PI) kullanıldı. Membran çözeltisi hazırlama sırasında kullanılan çözücü maddeler dimetilformamid (DMF) and tetrahidrofuran (THF)'dır. Karışık matrisli membranlar için aynı polimerler ile dolgu maddesi olarak kullanılan 60 nm boyutundaki ZIF-8 kristaller kullanıldı. ZIF-8 yüksek gaz adsorplama kapasitesine, iyi kimyasal ve ısıl kararlılığa sahiptir. Polimer harmanlı

membranlar PES/PI/20/80, PES/PI/50/50 and PES/PI/80/20 oranlarında hazırlandılar. Karışık matrisli membranlar ise aynı polimer oranlarına 10% ZIF-8 dolgu maddesi eklenerek üretildi. Polimer harmanlı ve karışık matrisli membranların H_2, CO_2 and CH_4 geçirimlilikleri sabit hacim-değişken basınç yöntemi kullanılarak tek gaz geçirgenlik sisteminde 35 °C'de ölçüldü. Geçirgenlik sonuçlarına göre, H_2/CO_2, CO_2/CH_4 and H_2/CH_4 ideal seçicilikler hesaplandı. Ayrıca, üretilen membranların CO_2/CH_4 karışım ayırma performansları ölçüldü. Besleme ve süzüntü gazını analiz etmek için gaz ayırımı ölçüm sistemi gaz kromatograf cihazına bağlandı.

Anahtar kelimeler: polietersülfon, poliimid, ZIF-8, polimer harmanlı membran, karışık matrisli membran

To my family

ACKNOWLEDGEMENTS

TABLE OF CONTENTS

LIST OF TABLES

LIST OF FIGURES

FIGURES

CHAPTER 1

INTRODUCTION

World population is expected to increase from 6.8 billion in 2010 to 9.2 billion in 2050 [1]. This expansion causes an equivalent increase in the overall energy consumption of world population from 15 TW to more than 40 TW [1]. The fossil fuels are the most preferred energy sources needed all around the world. However, due to the environmental problems caused by fossil fuels and their limited reserves, the research has focused on renewable and more efficient energy sources in recent years. One of the renewable energy sources is biogas which is obtained from plant, animal and industrial wastes.

The composition of biogas, which changes depending on the source used to produce it, is 50-75% methane, 25-45% carbon dioxide, 2-7% water vapor, <2% oxygen, <2% nitrogen, <1% ammonia, <1% hydrogen and <1% hydrogen sulphide in volume [2]. Methane is the desired component in the biogas and thus, the other components that reduces the energy density of biogas should be separated.

There are many separation methods such as cryogenic distillation, adsorption, amine absorption and membrane separation which are commonly used to separate CO_2 from CH_4 [1]. Although the most developed commercial technology among these separation methods is amine adsorption, it has some drawbacks such as high energy consumption for solvent regeneration, equipment or pipelines corrosion and flow problems due to viscosity change [1]. The membrane separation has several advantages over the other separation methods in terms of economical and operational issues. It has low operational and capital cost, ease of operation and low energy consumption. Besides membrane separation processes are proper to use in the systems, which does not need to very high purity and therefore it is possible to use membranes for biogas purification.

1

Membranes are semi permeable barriers which permeate some components faster than the others due to a driving force such as concentration or pressure gradients. In membrane separation processes, the components which permeate through the membrane are called as permeate and the components which are rejected by the membrane are called as retentate (Figure 1.1).
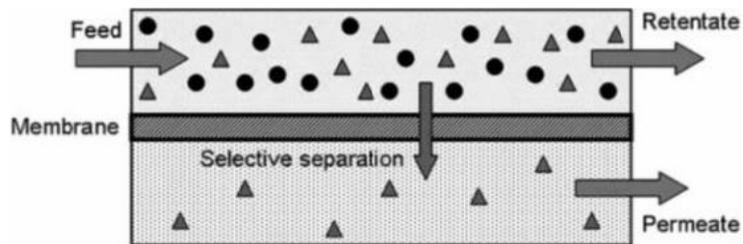
Figure 1.1 The schematic representation of feed, permeate and retentate of membrane [3]

The membranes can be categorized by symmetric and asymmetric in the way of their morphological structure. While the symmetric membranes are categorized as porous, non-porous (dense) and electrically charged membranes, the asymmetric membranes are classified as Loub-Sourirajan, thin-film composites and supported liquid membranes [4].

Isotropic microporous membranes have a highly voided structure and their pores, whose sizes are in the range of 0.01 to 10 μm in diameter, are randomly distributed and interconnected [4]. If the sizes of all particles in the feed are larger than the largest pore of the membrane, it is completely rejected. If some particles are smaller than the largest pores of the membrane and some particles are larger than the smallest pores, partially rejection occurs across the membrane. Particles, which are smaller than the smallest pores, completely permeate through the membrane. This type of membranes are generally used to separate the molecules which have different sizes in ultrafiltration and microfiltration [4]. Nonporous (dense) membranes consist of a dense film and the separation of various mixture components is determined by their diffusivity and solubility in the membrane film. They are mostly used for gas separation, pervaporation and reverse osmosis [4]. Asymmetrical membranes consist of a very thin surface layer and much

thicker porous substructure [4]. These two different parts of the membrane can be produced in separately or in one production process. The membranes whose thin surface layer and porous substructure are formed in separate operations are called as composite membranes and their layers are generally produced by using different polymers [4].

The permeability and selectivity shows separation performance of membrane. For the asymmetric gas separation membranes, permeance term is used instead of permeability because the permeance is independent of the membrane thickness.

The membrane permeance is defined as given below:

$$Permeance = \frac{Molar\ Flux}{Driving\ Force} \tag{1.1}$$

The driving force is generally the concentration difference between the feed and permeate sides of membrane. The unit of permeance is commonly used as gas permeation unit (GPU) and it is

$$1\ GPU = 10^{-6} cm^3(STP)/cm^2.s.cmHg \tag{1.2}$$

The permeability of a membrane can be defined as shown in Equation 1.3.

$$Permeability = Permeance \times membrane\ thickness \tag{1.3}$$

Ideal selectivity and selectivity (separation factor) are the other important terms to show the gas separation performances. Ideal selectivity of the membrane can be calculated by using the single gas permeances and membrane selectivity (separation factor) is based on permeate and retentate compositions. Ideal selectivity and selectivity (separation factor) are given in Equation 1.4 and Equation 1.5.

$$Ideal\ Selectivity_{A/B} = \frac{Permeance\ of\ A}{Permeance\ of\ B} \qquad (1.4)$$

$$Selectivity\ (separation\ factor) = \frac{\left[\frac{X_A}{X_B}\right]_{permeate}}{\left[\frac{X_A}{X_B}\right]_{retentate}} \qquad (1.5)$$

It is desired that a gas separation membrane has high permeability and selectivity for being usable for industrial applications. In general, while highly permeable polymeric membranes have low selectivity, highly selective membranes have low permeability. Robeson revealed the gas separation performance of polymeric membranes and a tradeoff between permeability and selectivity. The tradeoff curve of CO_2/CH_4 pair with prior and present upper bound is given in Figure 1.2:
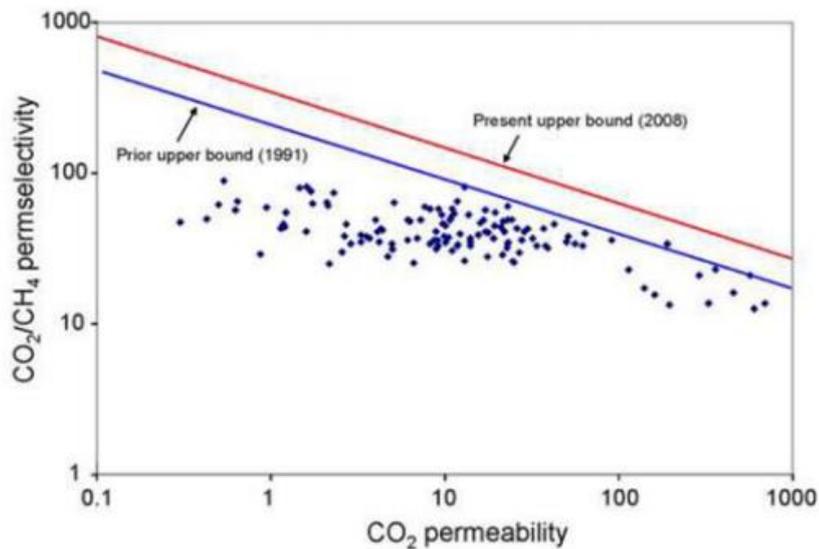
Figure 1.2: Robeson's tradeoff curve for CO2/CH4 pair [3]

The relationship between permeability and selectivity of the membrane is inversely proportional, that is, while the permeability increases, the selectivity decreases. The membranes, which are highly selective and low permeable, have no industrially usability. Thus, the production of highly selective and permeable

4

membranes is very important in terms of industrial applications. According to the Robeson's plot (Figure 1.2), the gas separation performances of the present polymeric membranes remain under the upper bound and these membranes cannot show the desired performance in terms of permeability and selectivity. Thus, many studies which are carried out for polymeric gas separation membranes are related with improving these membranes for exceeding the upper bound.

There are mainly four types of membranes for gas separation based on membrane materials which are polymeric membranes, inorganic membranes, facilitated transport membranes and mixed matrix membranes [5]. Polymeric membranes can be classified as rubbery or glassy which depends on both glass transition temperature of the polymer and operation temperature. While the rubbery membranes operate above the glass transition temperature, the glassy membranes operate below [6]. Polymer blending is a method by using different polymers with different properties in order to improve the performance of polymeric membranes. Inorganic membranes have better separation rate, thermal and chemical stability and efficiency compared to polymeric membranes but they are expensive, hard to handle and process. Therefore, these membranes are preferred in small scale applications [5]. Facilitated transport membranes is based on a chemical reaction which occurs between interested gas and membrane component, that is, carrier [6]. These membranes have high selectivity and maximum flux but they have also some disadvantages like mechanical stability, low diffusivity and defect formation [5]. Mixed matrix membranes have hybrid characteristics by combining organic and inorganic membranes. These membranes have good separation efficiency, cost effectiveness and thermal and mechanical stability [5].

The membrane performance in terms of gas separation is directly related with the intrinsic physicochemical properties of used polymeric material. During the polymeric materials selection, the gas permeability and selectivity coefficients, mechanical strength, glass transition temperatures, critical pressure of plasticization, material availability and the cost of a polymeric membrane material are taken into consideration [7].

5

In order to produce highly permeable and selective gas separation membranes, an improved method is the polymer blending which provides to produce enhenced polymeric membranes by combining different polymers rather than using only one type of polymer. Polymer blending is good preference due to simplicity and reproducibility [7].

Mixed matrix membranes, which are obtained by adding filler materials to polymeric membranes, are also developed in order to increase the gas separation performance. Potantial approach in mixed matrix membranes is to combine the advantages of inorganic and polymeric membranes. In mixed matrix membranes, the zeolites with aluminosilicate structure were generally used as filler materials. In recent years, nanoporous crystals which have metal organic frameworks (MOFs) have been used as filler material in membranes for gas separation. Because of their organic farmeworks in addition to porous structure like zeolites, they may be more compatible with polymers and thus, they may have high gas separation performance.

At this study, asymmetric polymer blend membranes and mixed matrix membranes are produced by using water vapor induced phase inversion method and their gas separation performances are investigated. During the membrane preparation, dry phase inversion was carried out by using infrared light with different time range and the effect of IR on gas separation was observed. Polyethersulfone (PES) and polyimide (PI) were used as polymer in order to prepare polymeric blend membranes. In mixed matrix membranes, while the PES and PI was still used as polymer, zeolitic imidazole framework-8 (ZIF-8) was used as filler material.

CHAPTER 2

LITERATURE RESEARCH

2.1. Polymeric Gas Separation Membranes

Increasing economical efficiency and extending the industrial usage of membrane separation processes depends on the improvement of highly selective and permeable membranes. Higher permeability provides to reduce the membrane area which is required to a given amount of feed gas and decrease the membrane capital cost. Moreover, higher selectivity of the membrane increases the purity of the products [3]. The polymeric membranes has been generally preferred to use in gas separation processes because they are available materials to produce good gas separation membranes. Commercial gas separation membranes are mostly produced by using polysulfone (PSf), polycarbonate (PC), cellulose acetate (CA), polyphenylene oxide (PPO), aramid and polyimide (PI). The polymeric membranes can be classified as symmetric (isotropic) and asymmetric (anisotropic) in terms of their pore structures and skin layers which are shown in Figure 2.1:
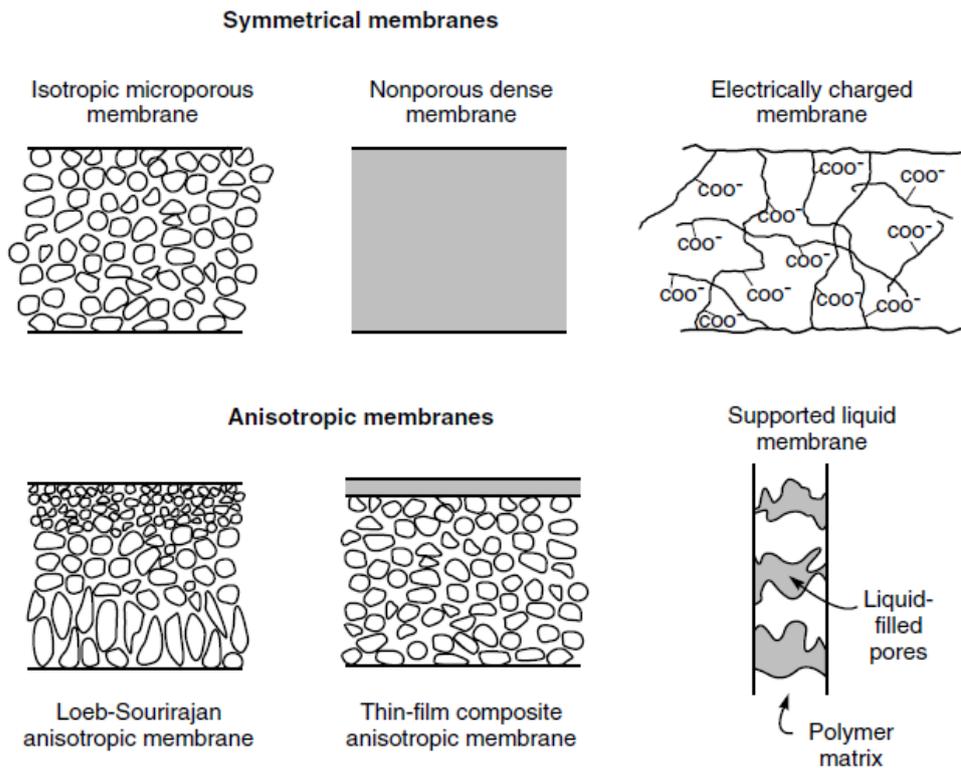
Figure 2.1 The schematic representation of the principal types of membranes [5]

Gas transportation is explained by solution diffusion model throughout the dense gas separation membranes. According to this model, feed gas is firstly dissolved in the membrane surface exposed to high gas pressure and then, it diffuses into the polymer matrix. After that, it is desorbed from the membrane surface exposed to low gas pressure [9].

The preparation of asymmetric membranes is based on the principle of the solvent-nonsolvent exchange in the phase inversion theory. During this process, while the solvent spreads through out of the polymer matrix, the non solvent diffuses into the polymer matrix. Solvent/non-solvent exchange causes to form porous asymmetric structure in the membrane matrix. A ternary diagram is used in order to explain phase inversion for a polymer, solvent and non-solvent system [10]. A common figure for ternary phase diagram is given in Figure 2.2.
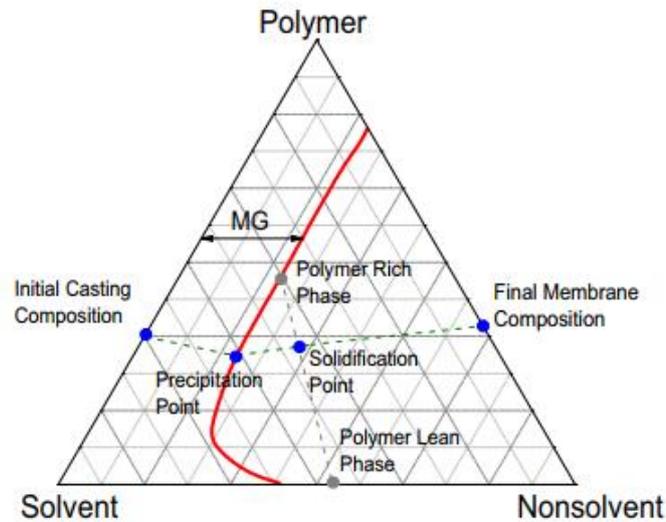
Figure 2.2 Schematic ternary system phase diagram [10]

The ternary diagram is separated into two parts which are single phase region and two phase region by binodal curve. In the single phase region, all of the components are miscible and miscibility gap (MG) is shown in this region of ternary system. Miscibility gap can be defined as the distance between polymer-solvent line and binodal curve and it quantifies the thermodynamic properties of casting solution [10]. In the two phase region, the ternary system divides into polymer rich (solid) and polymer lean (liquid) phase from solidification point [10]. The whole process is represented as a path on ternary diagram in Figure 2.2. The precipitation process starts with initial casting composition and it continues until the final membrane compositions. Precipitation point is called as the point at which polymer starts precipitating. When the composition proceeds and it reaches to the solidification point, the viscosity of the precipitated polymer becomes very high as solid [10]. The drawing tie line from solidification point identifies the polymer rich and polymer lean phases. While polymer rich phase represents the polymer matrix, polymer lean phase represents the pores [10]. The morphology of the produced membrane by phase separation is directly related with initial casting composition, followed precipitation path and binodal curve on the ternary system [10].

During the phase separation, the type of the non-solvent is crucial issue in terms of membrane morphology, gas permeance and gas separation performance. In

9

order to compare the effect of non-solvent on membrane characteristics and performance, two different study which have the same polymer and solvent during the membrane production were explained below.

Park et. al. studied on asymmetric polysulfone membrane produced by water vapor induced phase inversion [11]. During the membrane formation, while dry phase inversion was conducted by water vapor, wet phase inversion was carried out by N-methyl-2-pyrrolidone (NMP). The dry phase inversion occured in the membrane casting atmosphere which has the relative humidity of over 65%. The membrane morphology was investigated at different relative humidity (RH) values by a scanning electron microscope. The image which have RH 80% was given in Figure 2.3.
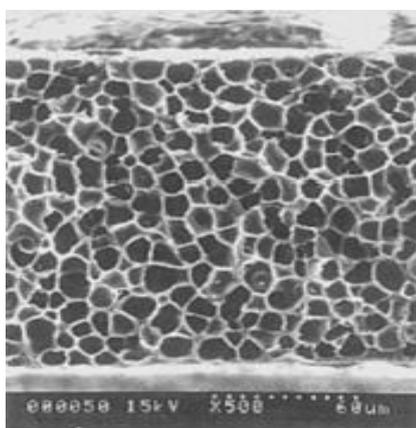
Figure 2.3 SEM image of PSf membrane for RH 80 % [11]

As seen in Figure 2.3, the PSf membrane made by water vapor induced phase inversion at RH 80% has the sponge like structure and symmetric cross-sectional morphology. In general, the membranes which are produced with liquid medium has the asymmetric structure [11]. The difference between the morphological properties of these membranes can be related with the kinetics instead of thermodynamics because thermodynamic status are the same for other components in the membrane [11]. Moreover, the effect of the RH% on pore size of the membranes were analyzed. According to this analysis, when RH% increases during the membrane formation, the pore size of the membrane decreases [11].

Blanco et.al. carried out a study about polysulfone membranes formation by wet phase inversion and their morphology [12]. Membrane formation was performed by using NMP as solvent and water as non-solvent during the phase inversion process. SEM analysis was used for the determination of PSf membrane morphology. The SEM photograph of this membrane cross-section by coagulating in water was shown in Figure 2.4:
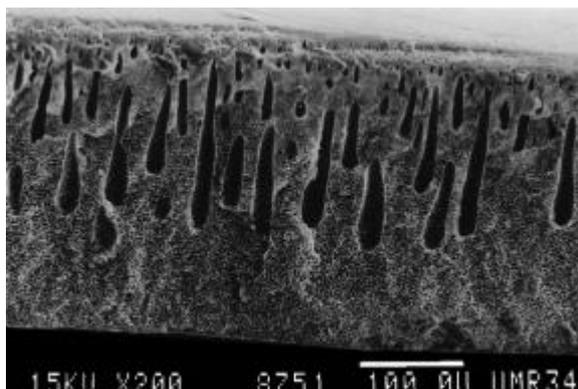
Figure 2.4 The cross-sectional SEM image of PSf membrane produced by coagulating in water by wet phase inversion [12]

According to the SEM image in Figure 2.4, PSf membrane produced by coaguating in water by wet phase inversion has small and numerous finger like pores under the selective skin layer. There are honeycomb-like structure between these pores of the membrane [12].

2.2. Metal Organic Frameworks

Mixed matrix membranes are produced by using different types of nanofillers such as fumed silica and other silicon containing particles which are the most common filler materials. Other nanoparticles can be mainly classified as carbon molecular sieves, TiO, MgO, zeolites and metal organic frameworks (MOFs) [13]. While the fumed silica, TiO and MgO are solid and impermeable, zeolites and MOFs are porous and permeable nanofillers [13]. Among them, MOFs are particularly more attractive nanoporous materials. They are class of porous crystalline materials and they are consists of metal ions linked by organic bridging ligands [14]. MOFs have distinct properties like high porosity and

flexilibility. Morever, they have very large pores which are larger than 1 nm and thus, they can be penetrated by polymer chain in MMMs [14].

2.2.1. Zeolitic Imidazolate Framework-8 (ZIF-8)

Zeolitic imidazole frameworks (ZIFs) are porous crystals and they are new, subclass of metal organic frameworks. They have remarkable properties such as permanent porosity, good thermal and chemical stability etc. for many applications like separation prosesses [15]. ZIFs structure can be represented as T-Im-T with an angle of 145°. This angle is very close to the characteristic Si-O-Si angle in zeolites [16]. While T represents tetrahedral metal ion, Im shows imidazolate or a derivative. Zeolitic imidazole framework-8 (ZIF-8) is commonly known and special type of ZIFs with sodallite (SOD) topology [16]. The crystalline structure of ZIF-8 is schematically given in Figure 2.5:
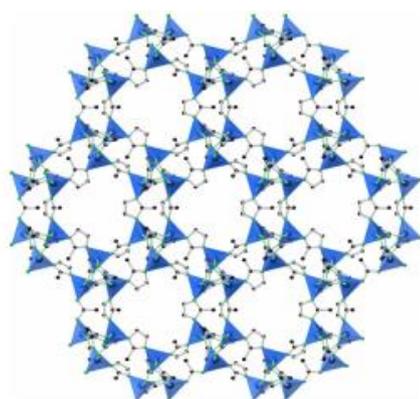
Figure 2.5 The schematic structure of ZIF-8 [13]

ZIF-8 shows high thermal and chemical stability compared to many other MOFs. They have high surface area (1300-1700 m^2/g) and good thermal stability (up to 450 °C) [13].

2.3. Asymmetric Polymeric Blend Membranes

Han et. al. studied on flat sheet gas separation membranes of polyethersulfone (PES), polyimide (PI) and their blends [17]. They produced these membranes by using spin casting method and dry/wet induced phase inversion method. The blend compositions of polymers were varied from 90/10 to 10/90. While the

NMP was used as solvent, water was used as non-solvent. Moreover, DMF was also used in order to observe the effects of solvents on the membrane cross-section morphology. Mixing compatibilities and thermal stabilities of the produced membranes were studied by Fourier Transform infrared spectroscopy (FTIR) and thermal gravimetric analysis (TGA). Moreover, scanning electron microscopy (SEM) was used in order to analyze the the produced membrane morphology. The gas permeation tests were performed for H_2, O_2 and N_2 gases. The SEM photographs of the membrane cross-sections for different blend compositions are shown in Figure 2.6.
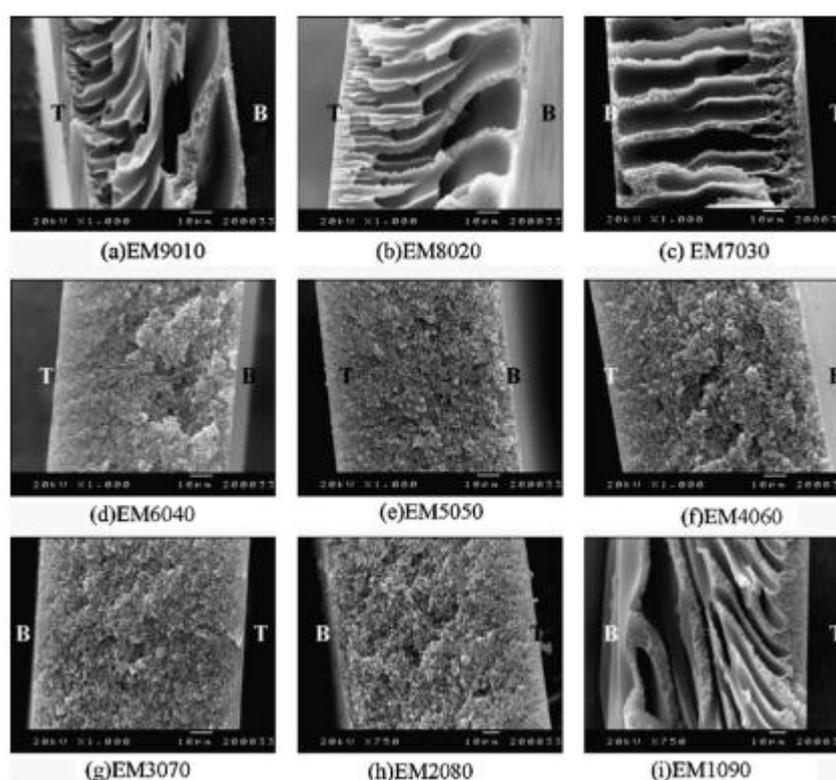
Figure 2.6 The SEM images of membrane cross-sections for different blend compositions [17]

According to Figure 2.6, the morphologies of the membranes which have the blend ratios of PI between 40 and 80 wt.% showed the microporous sponge-like structure. On the other hand, an asymmetric finger-like structure was observed in image (c) in Figure 2.6 [17]. In order to investigate the effects of solvent, DMF was used as solvent instead of NMP and the blend compositions of PES/PI 80/20,

60/40, 40/60 and 20/80 were chosen. For these blend membranes, cross-section images by SEM are given in Figure 2.7.
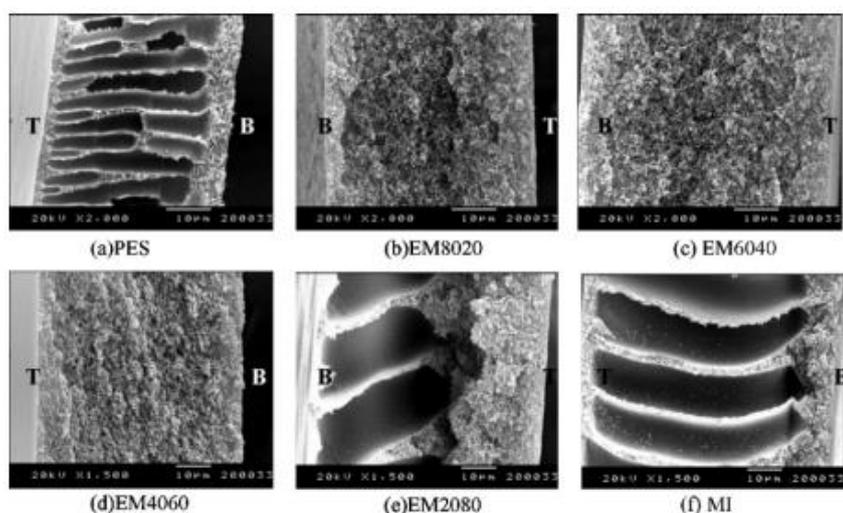
Figure 2.7 The SEM images of membrane cross-sections for different blend compositions by using DMF [17]

According to Figure 2.7, the membrane morphologies which have the blend ratios of PI between 20 and 60 wt.% showed sponge-like structure. Eventually, it can be determined that blend polymer-solvent interaction is stronger in the case of DMF than that case of NMP [17]. According to the gas permeation tests, it was seen that H_2, O_2 and N_2 permeabilities increased with increasing feed pressure increases for all the blend composition. Moreover, when the amount of PES increased in the blend composition, N_2 gas permeance also increased [17].

Another research, which was conducted by Rafiq et. al. was on asymmetric polysulfone (PSf)/polyimide (PI) blended membranes by phase inversion method [18]. The compositions of blends were changed at compositions of 80/20, 50/50 and 20/80 for N-methyl-2-pyrrolidone/dichloromethane (DCM/NMP). DCM/NMP was used as solvent mixtures in order to determine CO_2/CH_4 separation performance of the membrane [18]. Moreover, ethanol was used as non-solvent during the membrane preparation by phase inversion. The gas permeation tests of the blend membranes were performed in the range of 2-10 bar. The cross-sectional images of PSf/PI-20% membranes with DCM/NMP 80/20, 50/50 and 20/80 are represented in Figure 2.8.
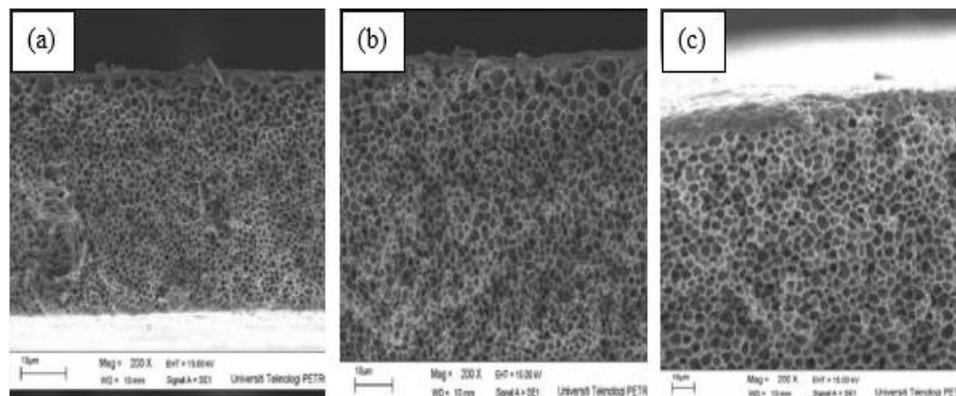
Figure 2.8 SEM photographs of PSf/PI-20% membranes with DCM/NMP (a) 80/20, (b) 50/50 and (c) 20/80 [18]

According to the SEM images given above, membranes which was prepared by using different solvent mixtures has sponge-like substructures. Moreover, the membrane prepared by using DCM/NMP 80/20 has thin skin layer and smaller pore sizes. This demonstrated that low boiling DCM solvent provided to reduce the skin structure and NMP solvent controlled the rate of evaporation which causes delayed demixing [18]. According to the thermal gravimetric analysis on the produced blend membranes, when the amount of PI increased in the blend composition, the glass transition and decomposition temperatures also increased. Moreover, the effects of different solvent ratios on the membrane CO_2 and CH_4 permeances were studied. It was seen that when the DCM composition in the DCM/NMP solvent mixture decreased, CO_2 and CH_4 permeation increased. Also, when the operating pressure raised from 2 bar to 10 bar, permeance values of the membranes decreased and PSf/PI-20% membrane has the highest selectivity of 28.70-28.22 in the pressure range [18].

Basu et. al. studied on another asymmetric blend membranes in order to achieve enhanced permeance and stability in CO_2/CH_4 mixture separation [9]. For thist study, Matrimid® (PI) and Ultrason polysulphone (PSf) were used with different blending ratios and they were produced by using phase inversion method. During the production, NMP/1,3-dioxalane solvent mixture was used with different ratios and water was used as non-solvent. Physical properties of the produced membranes like glass transition temperatures (T_g), density and d-spacing were analyzed and the calculated values are tabulated in Table 2.1:

Table 2.1 Physical properties of the produced membranes [9]

Membrane Type	T_g (°C)	Density (g/cm³)	d-spacing (Å)
PI	337	1.170	5.70
PI/PSf/1/3	197	1.220	4.95
PI/PSf/1/1	221	1.203	5.03
PSf/PI/3/1	309	1.186	5.23
PSf	187	1.240	4.86

Their SEM images were obtained in order to better understanding membrane cross-section morphology. According to the SEM results, it was seen that the produced membranes have porous substructure, which consists of macrovoids, and it was covered by thin, dense selective skin layer [19]. Moreover, CO_2/CH_4 gas mixture selectivities were measured with different CO_2 amount in the feed for PI, PSf and PI/PSf blend membranes at constant temperature. It was seen that when the amount of CO_2 in the feed composition increased, the membrane selectivities decreased. In addition, temperature dependence of the produced membranes on CO_2/CH_4 gas mixture selectivity were studied. When the temperature increased from 35°C to 95°C, the membrane selectivities decreased. According to the results, PI selectivity goes below the blend membrane selectivity at above 65°C. However, the selectivity of the blend membranes increase very slowly during the temperature falling [19]. Pressure dependency of the produced membrane on CO_2/CH_4 gas mixture performance was also investigated. For this purpose, feed pressure changed from 4 bar to 14 bar and the feed composition stayed constant at 75/25 vol% CO_2/CH_4 mixture. It was observed that the membrane selectivities increased with increasing the feed pressure. While the blend membranes showed constant selectivity rise with higher pressures, PI selectivity increased up to 12 bar and it started to suddenly decrease [19].

Kapantaidakis et. al. studied on polyethersulfone Sumikaexcel (PES)/polyimide Matrimid 5218 (PI) blend gas separation hollow fiber membranes for the compositions of PES/PI 80/20, 50/50 and 20/80 [20]. In order to prepare

asymmetric hollow fiber membranes, dry/wet spinning process was applied by using blends of two polymers. During the phase inversion process, NMP and water were used as solvent and non-solvent, respectively. The gas permeability performances of the produced membranes were performed for CO_2 and N_2 gases. Moreover, membranes were coated with polydimethylsiloxane (PDMS) and the effect of coating process on gas permeability performance were analyzed. When the air gap increased during the membrane preparation, membranes had porous skin layer, loose substructure and high permeances [20]. After coating, the CO_2 permeance of the membranes changed in the range of 31 – 60 GPU and their CO_2/N_2 selectivities varied from 40 to 35 [20].

Another study related with polymer blending technology was performed by Hosseini et. al. [21]. While Matrimid® and polybenzimidazole (PBI) were used as polymer for blending, polysulfone (PSf) was used for the coating to the inner layer of the membrane. In this study, the effects of change in some parameters like air gap and outer dope flow rate were analyzed on membrane performance. The produced membranes were tested with H_2, CO_2 and CH_4 gases in order to determine their gas permeabilities. According to the results, it was seen that air gap distance and spinning type are effective on gas separation performances of the membranes [21]. Moreover, CO_2/CH_4 separation performance raised with the increasing outer dope flow rate. SEM images of the membranes showed that while the Matrimid®/PBI blend layer had sponge like structure, the inner layer coated by PSf had finger like structure [21].

2.4. Asymmetric Polymer Blend Mixed Matrix Membranes

Basu et. al. investigated asymmetric polymer blend based mixed matrix membranes produced by using phase inversion method [22]. Matrimid® (PI) and polysulphone (PSf) were used as blended polymers and a crystalline metal organic framework (MOF), which is $Cu_3(BTC)_2$, was used as the filler material. During the membrane preparation, NMP/dioxalane mixture was used as solvent and water was used as non-solvent. The physical properties of the produced MOF and membranes, which are film density, glass transition temperature and d-spacing, were studied. SEM images were obtained in order to determine the

distibution of MOF into the polymer matrix by analyzing the membrane cross-section. Also, gas permeance tests of the produced membranes were performed for CO_2, CH_4 and N_2 gases and their selectivities were calculated. While the produced membranes contained 20 wt% polymer blends, MOF contents changed in 10, 20, 30 wt% compositions. In order to determine thermal properties, thermal gravimetric analysis were performed for PI and $Cu_3(BTC)_2$/PI mixed matrix membranes. According to the TGA results, decomposition temperatures of PI and $CU_3(BTC)_2$ are 487°C and 300°C, respectively. The thermal stability of MMMs increased due to the high thermal stability of $Cu_3(BTC)_2$ and interaction between the PI and $Cu_3(BTC)_2$ [22]. When the selectivities and permeances of the membranes were examined, it can be seen that filler material increased the membrane selectivity and permeance compared to the unfilled membranes. The SEM images of unfilled PI and PI/PSf membranes, and PI/ $Cu_3(BTC)_2$ – 30% coated with PDMS membrane were shown in Figure 2.9.
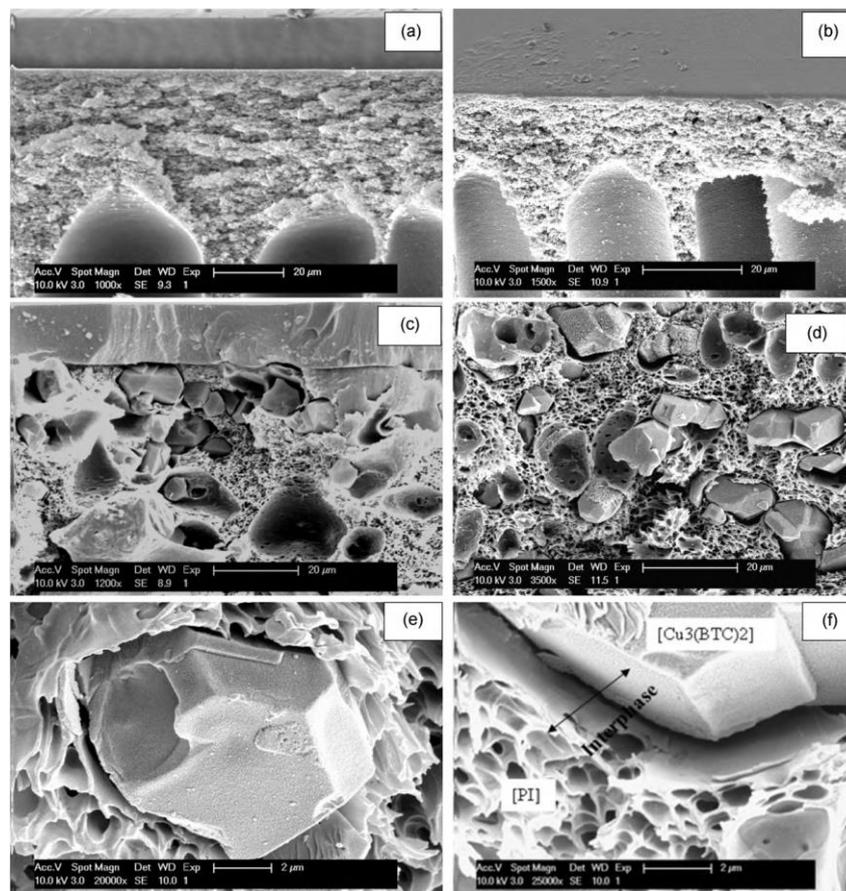
Figure 2.9 (a) unfilled PI membrane (b) unfilled PI/PSf/3/1 membrane (c) PI/Cu$_3$(BTC)$_2$-30% coated with PDMS (d) PI/Cu$_3$(BTC)$_2$-30% membrane at low magnification (e) PI/Cu$_3$(BTC)$_2$-30% membrane at high magnification (f) PI/Cu$_3$(BTC)$_2$ interface [22]

When looking at the image (a) and (b) in Figure 2.9, it can be seen that skin layer of the membranes are supported by a macro voided porous sub-layers. This part of the membrane provides to only mechanical support for the selective skin layer and it has no effect on the gas permeation or gas mixture separation [22]. The overall cross-section of the mixed matrix membrane with 30% loading is shown at image (c) in Figure 2.9. This photograph showed that the filler material embedded into the polymer matrix and they located under the skin layer. According to the image (d) in Figure 2.9, Cu$_3$(BTC)$_2$ crystals can be easily seen, that is, there is no agglomeration. Therefore, it can be said that filler materials are well dispersed into the polymer matrix. The image (e) and (f) in Figure 2.9 show the good contact at the filler/polymer interface. Moreover, the increasing CO$_2$ composition in the feed gas during the gas mixture separation caused to decrease

19

the CO_2/CH_4 and CO_2/N_2 selectivities of all produced membranes. The CO_2/CH_4 and CO_2/N_2 selectivity of PI/PSf/3/1 membrane is lower than that of PI/Cu_3(BTC)$_2$ and pure PI membrane [22].

Another study related with asymmetric polymer blend mixed matrix membranes were conducted by Rafiq et.al. [23]. In this study, polysulfone (PSf)/polyimide (PI) asymmetric membrane including inorganic silica nanoparticles as filler material was produced for CO_2/CH_4 mixture separation by using phase inversion method. During the membrane production, DCM/NMP mixture was used as solvent and ethanol was used as non-solvent. The produced blend MMMs were analyzed by using characterization techniques which are SEM, DSC and TGA. Moreover, the gas permeation and gas mixture separation tests were performed for CO_2 and CH_4 gases. According to SEM results, it is observed that the produced membrane surfaces are smooth and homogenous. This means that two polymers were compatible with each other [23]. Also, the addition of silica particles up to 15.2 wt% resulted in homogenously dispersion into the polymer matrix but silica content reached to 20.1 wt% caused to agglomeration in the matrix. DSC analysis was carried out in order to understand the effect of the silica particles on PSf/PI blend membranes. It is seen that when the amount of silica increased, glass transition temperature of the membranes also increased. It represents the good interaction between silica particles and polymers [23]. TGA results showed that the addition of silica into the polymer blends provided to improve thermal stability of the membranes. The weight loss of the membranes with heating was observed above 700 °C and thus, their thermal stabilities are very high [23]. Gas permeance tests were carried out in the range of 2-10 bar feed pressures. When the feed pressure was set to 10 bar, while the CO_2/CH_4 ideal selectivities of PSf/PI-20% and PSf/PI-20% + 15.2 wt% silica membranes were equal to 29.7 ± 0.6 and 60.2 ± 0.4, respectively [23]. Mixed gas selectivities of the same membranes were calculated for the composition of CO_2/CH_4 25/75, 50/50, 75/25% and they were found as nearly the same with ideal selectivity values.

CHAPTER 3

EXPERIMENTAL METHODOLOGY

3.1. PES/PI and PES/PI/ZIF-8 Membranes Preparation

3.1.1. PES/PI and PES/PI/ZIF-8 Membranes Materials

Polyethersulfone (Radel A-100) was purchased from Solvay. The molecular weight, density and glass transition temperature of PES are 53000 g/mol, 1.37 g/cm^3 and 220 °C respectively. Matrimid ® 5218 polyimide resin, whose molecular weight, density and glass transition temperature are 80000 g/mol, 1.2 g/cm^3 and 300 °C respectively, was provided by Alfa Aesar.
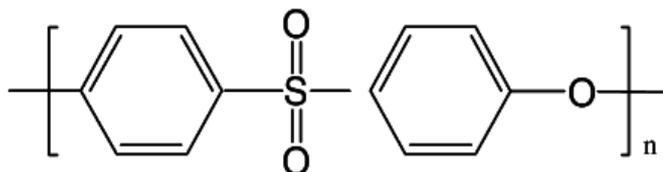
Figure 3.1 Molecular Structure of PES [24]
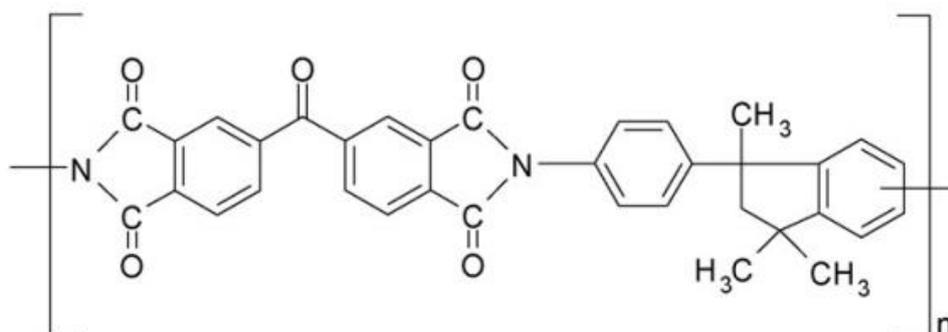
Figure 3.2 Molecular Structure of Matrimid ® 5218 polyimide [25]

In order to remove any absorbed atmospheric gas, polymers were dried at 80 °C in the oven at least for 1 night before membrane preparation. N,N-Dimethylformamide (DMF) and tetrahydrofuran (THF) were used as solvent. These solvents were purchased from Sigma-Aldrich. Water vapor was used as non-solvent during the membrane preparation.

3.1.2. Materials and Synthesis of ZIF-8

Zinc nitrate hexahydrate ($Zn(NO_3)_2.6H_2O$ with 98% purity), 2-methyl imidazole and methanol are chemicals to produce ZIF-8. Zinc nitrate hexahydrate was purchased from Across Organics. 2-methyl imidazole and methanol were bought from Sigma-Aldrich.

ZIF-8 crystals were produced by using the procedure which is explained in Keser Demir et. al.[26]. According to this method, 4.8 g zinc nitrate hexahydrate was firstly dissolved in 180.8 g methanol in a beaker. At the same time, 10.6 g 2-methylimidazole were dissolved in 180.8 g methanol in a different beaker. Following the vigorous mixing to obtain homogenous solutions, the solution including zinc nitrate hexahydrate was added to the imidazole solution to obtain synthesis mixture and the reaction was started for the production of ZIF-8. The crystallization has carried out at room temperature. This mixture was stirred for 1 hour at 300 rpm to complete the production of ZIF-8 crystals. Meanwhile the color of solution, which has initially transparent, turned into white. Following to crystallization, ZIF-8 crystals were separated from the mother liquor by centrifugation. In order to remove remaining zinc nitrate hexahydrate and 2-methyl imidazole, the precipitated ZIF-8 crystals were washed with methanol twice. After the washing procedure, the ZIF-8 crystals were dried at 80 °C in an oven overnight in order to remove any remaining methanol. ZIF-8 crystals were activated at 180 °C in an oven overnight before using for the membrane preparation.

3.1.3. Asymmetric Membrane Preparation Methodology

The homogenous polymer solutions of asymmetric PES/PI blend membranes were prepared from a solution containing 9.5 g DMF and 4 g THF as solvents and 4 g polymer. The ratio of PES/PI into the polymer solutions was different.

The polymers were dissolved in DMF and THF by priming. For example, to prepare PES/PI/20/80 blend membrane, first 0.8 g PES was dissolved into DMF and THF mixed solvents and then, 3.2 g PI was added to the PES-DMF-THF solution by priming and this mixture was stirred overnight. The solution was degassed for 15 minutes by using ultrasonic bath between each polymer addition to the solution in order to prevent agglomeration of the polymers. After a homogeneous solution was obtained, it was waited overnight in order to degas the solution before casting procedure. The procedure of polymer blend membrane was shown in Table 3.1.

Table 3.1 The method of polymeric blend membranes

Membrane Code	PES wt%	PI wt%	PES (g)	PI (g)	Total Amount of Solid (g)	Amount of DMF (g)	Amount of THF (g)
PES/PI/20/80	20	80	0.8	3.2	4	9.5	4
PES/PI/50/50	50	50	2	2.0	4	9.5	4
PES/PI/80/20	80	20	3.2	0.8	4	9.5	4

For the production of mixed matrix membranes, ZIF-8 crystals which are the 10% weight percent of the polymer were added to the DMF/THF solvent mixture. ZIF-8 crystals which are not annealed in order to prevent agglomeration of the ZIF-8 crystals were firstly washed with DMF solvent and then, added to the solvent mixture. The DMF/THF/ZIF-8 mixture was stirred milky overnight by magnetic stirrer. The polymer addition to the solution and the casting process of mixed matrix membrane were the same as the blend membrane preparation. The method of polymer blend based mixed matrix membranes was tabulated in Table 3.2.

Table 3.2 The method of mixed matrix membranes

Membrane Code	PES wt%	PI wt%	ZIF8 wt%	PES (g)	PI (g)	ZIF8 (g)	Total Amount of Solid (g)	Amount of DMF (g)	Amount of THF (g)
PES/PI/ZIF8 20/80/10	20	80	10	0.8	3.2	0.4	4	9.5	4
PES/PI/ZIF8 50/50/10	50	50	10	2.0	2.0	0.4	4	9.5	4
PES/PI/ZIF8 80/20/10	80	20	10	3.2	0.8	0.4	4	9.5	4

The air conditioning glove box shown in Figure 3.3 was used for the membrane casting process. The volume of the air conditioning glove box is approximately 40 L. It includes an infrared bulb with 250 watt power and automatic film applicator. There are three discharge pipes at the back cover of the box. One of the discharge pipes is used for blowing off the solvent vapor into the glove box. The other two discharge pipes were designed for the humidity control of the glove box. In order to humidify the air in the box, the air which was sucked from the glove box by fan was passed from a column which includes 750 ml water at 100 °C and humidified air was sent to the glove box again. The relative humidity of the glove box was measured by using hygrometer.

Figure 3.3 Air conditioning glove box

After the relative humidity of the glove box was set to the desired value, the membrane solution was cast into 500 µm thin film on glass plate by automatic film applicator. Then, the membrane film was exposed to the infrared light for dry phase inversion for 0 to 120 sec. After the dry phase inversion process was accomplished, membrane film was waited in the humid air until the film separated from the glass plate, which takes approximately 8 h, and wet phase inversion was completed. Finally, the membrane was placed in a vacuum oven which was set to 120 °C overnight in order to vaporize remaining solvent.

3.2. Characterization of Blend and Mixed Matrix Membranes and ZIF-8 Crystals

The produced blend and mixed matrix membranes were characterized by thermal gravimetric analysis (TGA), scanning electron microscopy (SEM), differential scanning calorimetry (DSC) and X-ray diffraction (XRD).

3.2.1. Thermal Gravimetric Analysis (TGA)

In thermal gravimetric analysis, weight loss of the membrane is determined with temperature at constant heating rate. Shimadzu DTG-60H TGA analyzer was used to determinate the thermal behavior of the blend and mixed matrix membranes. During the analysis, a small piece of membrane was used as sample and it was heated from 25°C to 650 °C with heating rate 10 °C/min. The experiment was performed under N_2 atmosphere.

3.2.2. Differential Scanning Calorimetry (DSC)

Differential scanning calorimetry was performed to determine the glass transition temperature of the produced blend and mixed matrix membranes. The analysis has carried out by Shimadzu DSC-60. In the sample chamber of the device, there were two aluminum pans which were sample pan and reference pan. While the sample pan contained the membrane sample, the reference pan was left empty. Then, the membrane sample was heated from 25°C to 350 °C with a heating rate of 10 °C/min under N_2 atmosphere.

3.2.3. Scanning Electron Microscopy (SEM)

The produced blend and mixed matrix membranes morphologies were determined by Scanning Electron Microscopy in METU Central Laboratory. The SEM analyses were performed by QUANTA 400F Field Emission series scanning device. During the preparation of the sample, a small piece of membrane was cut and dipped into liquid nitrogen in order to obtain a fractured membrane cross-section.

3.2.4. X-Ray Diffraction (XRD)

X-Ray Diffraction was used to determinate the crystallinity of produced ZIF-8 particles which was used as filler in the membrane. The analysis was performed by using Philips PW 1729 X-Ray Diffractometer, with Cu-Kα tube at 30 kV voltage and 24 mA current, and 0.05 %/min scan rate for Bragg angles between 5-40°. The XRD patterns of the ZIF-8 particles were compared with the patterns give in the literature.

3.3. Gas Permeation Measurements of Blend and Mixed Matrix Membranes

Gas permeation measurements through the blend and mixed matrix membranes were conducted by using the gas permeation system (*Figure 3.4*), which was designed and set in the laboratory. It was designed based on both constant volume-variable pressure method and constant pressure-variable volume method but the measurements were only performed by using constant volume-variable pressure method. The system was set by using pneumatic polyurethane tubings and two way-three way Aignep valves. There are two membrane modules (Membrane module A and B) which are suitable for the flat membranes with effective membrane area of 13.2 cm^2. In order to prevent any gas leakage from membrane modules, two Viton O-Rings were placed on the membrane cell. According to system, two different membranes can be vacuumed and tested simultaneously. The membrane modules are placed in a temperature controlled forced connective oven. Pt-100 type thermocouple is used to measure the oven

temperature. A two-stage rotary vacuum pump (Edwards) was used in order to vacuum the feed and permeate sides of the membranes.
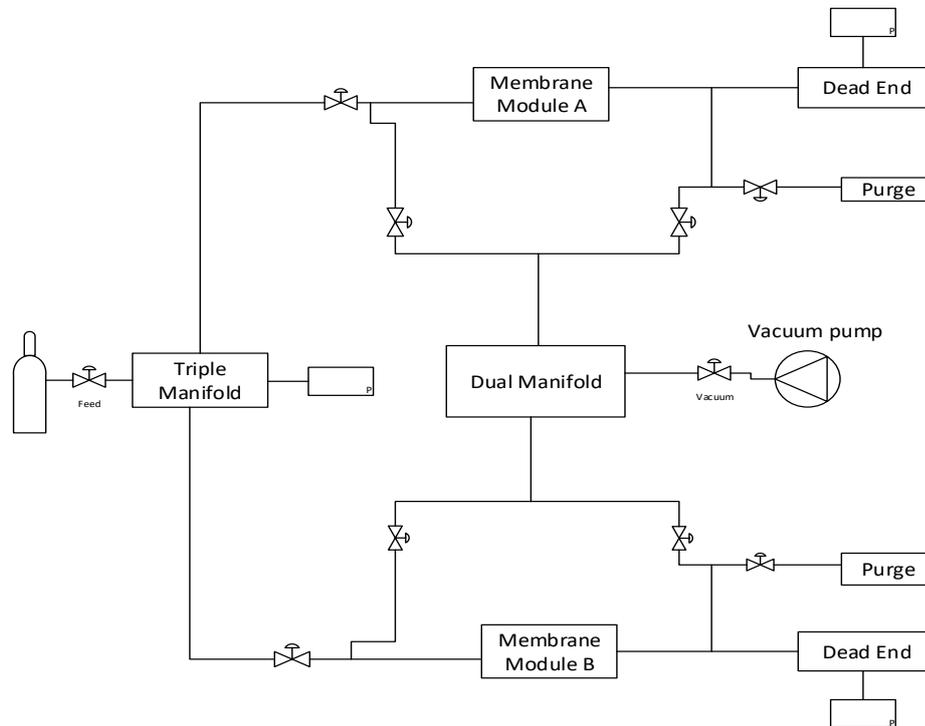
Figure 3.4 Single Gas Permeation Test System

Gas permeation measurements were performed at 3 bar transmembrane pressure and 35 °C. Firstly, a piece of membrane with area of 16.6 cm^2 was cut and put into the membrane module. Then, the feed and permeate sides of the membrane were vacuumed for approximately 1 hour in order to desorb air or remained gas from the previous tests. After that, while the permeate side was in vacuum, the feed pressure was adjusted to 2 bar (3 bar transmembrane pressure). The pressure rise in the permeate side was measured with time by a pressure transducer and the data was recorded to the computer by DaLi08 Data Acquisition and Logging Interface. H$_2$ (Linde, 99.99%), CO$_2$ (Linde, 99.99%) and CH$_4$ (Linde, 99.95%) were used during the gas permeation measurements.

3.4. Mixed Gas Separation Measurements of Blend and Mixed Matrix Membranes

The CO$_2$/CH$_4$ mixtures were separated by blend and mixed matrix membranes using constant volume-variable pressure method. The system (Figure 3.5) was

designed and set in the laboratory like gas permeation measurement system. Experimental setup includes a gas tank, membrane module, pressure gauge, pressure transmitter, computer, heating tape, temperature controller and vacuum pump. Also, the system was directly connected to a gas chromatography in order to analyze feed and permeate gases. All of the components of the system which are piping, fittings, membrane module and feed gas tank were made from stainless steel. The feed gas tank was designed as seamless stainless steel to be durable for high pressures. The piping and fittings which have ¼'' diameter were bought from Hoke and Swagelok. The membrane module with an effective membrane area of 9.6 m^2 was purchased from Millipore (part no. XX45047 00). In order to prevent any gas leakage from the membrane cell during the experiment, two Viton O-Rings were used and placed on the cell. The pressure change at the permeate side was measured by using MKS Baratron pressure transducer (0-1000 Torr $\pm$ 0.1 Torr) and the data were recorded by computer. All parts of the system was evacuated by using two-stage rotary vacuum pump. The temperature of the system was adjusted by using a heating tape and J type thermocouple was used in order to measure system temperature.
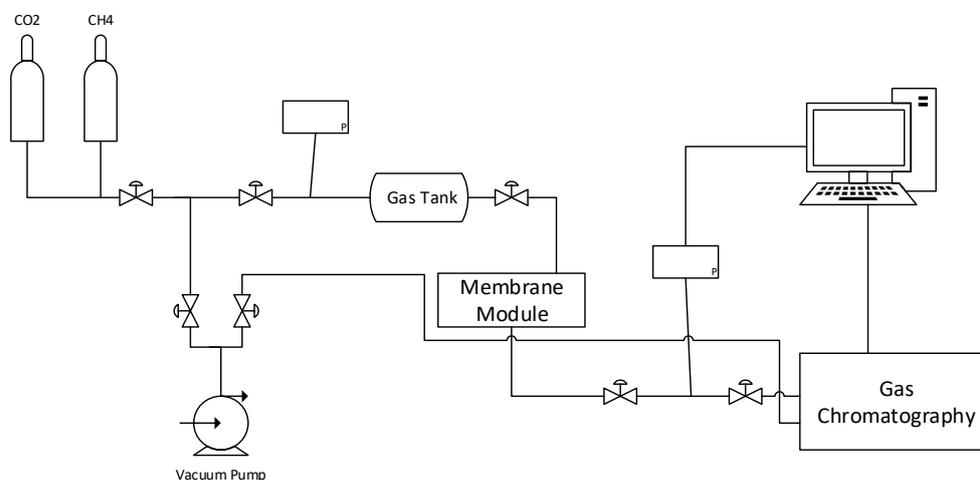
Figure 3.5 Mixed Gas Separation System

In gas separation measurements, CO_2/CH_4 mixtures which include CH_4 gas with volume percents of 30%, 50% and 70% were used as feed gas to the membrane. The measurements were carried out with 3 bar transmembrane pressure and difference at temperatures between 35°C and 90°C. The used CO_2 (Linde,

28

99.99%) and CH_4 (Linde, 99.95%) has high purity. Before starting to the experiment, a piece of membrane with 16.6 cm^2 was cut and placed into the membrane module and the desired temperature value was set. At the same time, all part of the system was evacuated. The membrane should be vacuumed at least 1 hour before the experiment in order to remove remaining gas. Initially, the permeate side of the membrane was under vacuum (approximately 5 Torr) and the feed side was adjusted to 2 bar with desired mixture composition of CO_2/CH_4. The pressure difference between feed and permeate sides of the membrane provides driving force of the separation process. After the measurement was started, the increase of pressure in the permeate side was measured against time. When the permeate pressure reached to approximately 100 Torr, the mixture in the permeate side was sent to gas chromatography for composition analysis.

In gas chromatography, Chromosorp 102 (80-100 mesh) type column and TCD detector were used. Before the measurements, the GC was calibrated and calibration curves (peak area versus pressure) were obtained by analyzing pure CO_2 and CH_4 gases at certain pressure values. Operating conditions of GC were tabulated in Table 3.3.

Table 3.3 Operating Conditions of Gas Chromatography

GC Properties	Operating Conditions
Column Temperature	80 °C
Column Pressure	30 psi
Detector Temperature	100 °C
Valve Temperature	80 °C
Reference Gas	Helium
Total Flow Rate	50 ml/min

The calibration curves of CO_2 and CH_4 gases were given in Appendix B. Moreover, a sample calculation for permeance and selectivity of CO_2/CH_4 mixture was shown in Appendix A.

CHAPTER 4

RESULTS AND DISCUSSION

4.1. Characterization of ZIF-8 Crystals

ZIF-8 crystals were synthesized and used as filler material in mixed matrix membranes. ZIF-8 was characterized in terms of crystallinity and morphology and pore structure by using XRD, SEM and BET.

The ZIF-8 particles were analyzed by using XRD in order to determine their crystallinity. Before analysis, they were dried at 80 °C overnight. Then, they were crushed in a mortar and put into an oven at 180 °C overnight to activate the powder. The activated ZIF-8 powder was analyzed by XRD and the results were compared with reference values.

The XRD patterns for ZIF-8 particles produced in two different synthesis and reference pattern [26] were given in Figure 4.1.
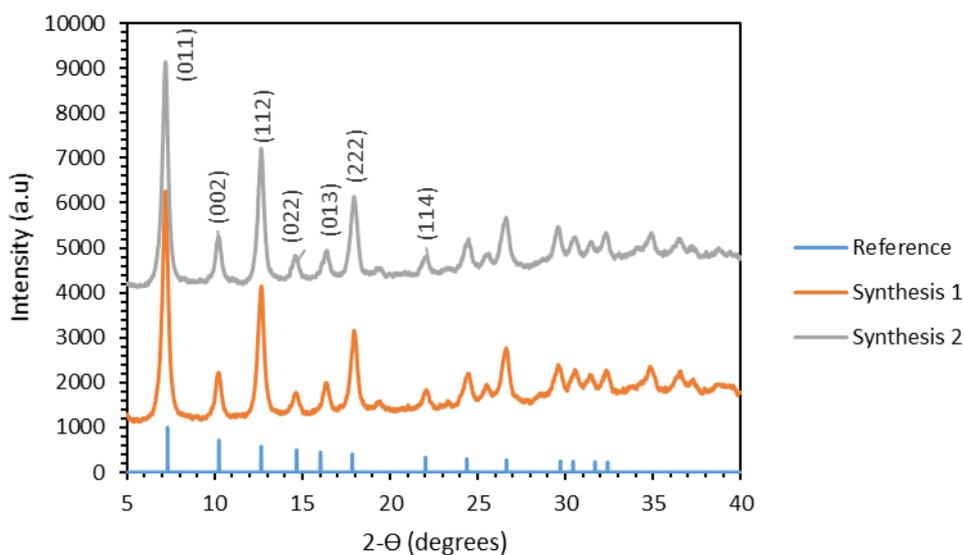
Figure 4.1 X-Ray Pattern of ZIF-8 crystals and reference pattern [26]

According to the XRD patterns in Figure 4.1, the characteristic peaks of the produced ZIF-8 crystals and that of reference sample were matched at the same 2-Θ angles. This means that the synthesis of ZIF-8 crystals were successfully completed.

The area under the characteristic diffraction peaks on the XRD pattern of the ZIF-8 crystals provides the crystallinity of the ZIF-8 crystals. The peak areas under the characteristic peaks and total peak area of the synthesized ZIF-8 crystals were given in Table 4.1.

Table 4.1 Peak Areas under the characteristic peaks of Synthesized ZIF-8 crystals

Planes of Peaks	Areas of Peaks	
	Synthesized 1	Synthesized 2
(011)	1547	1418
(002)	204	127
(112)	883	846
(022)	95	117
(013)	154	125
(222)	563	541
(114)	49	60
Total Peak Area	3495	3234

In Table 4.1, it can be seen that the total peak areas of the synthesized ZIF-8 crystals are very similar. Therefore, it can be said that the reproducible ZIF-8 crystals were synthesized.

The morphology of the synthesized ZIF-8 crystals was performed by using scanning electron microscopy (Figure 4.2). The synthesized ZIF-8 crystals are well dispersed and have hexagonal shape coherent with the literature [27].
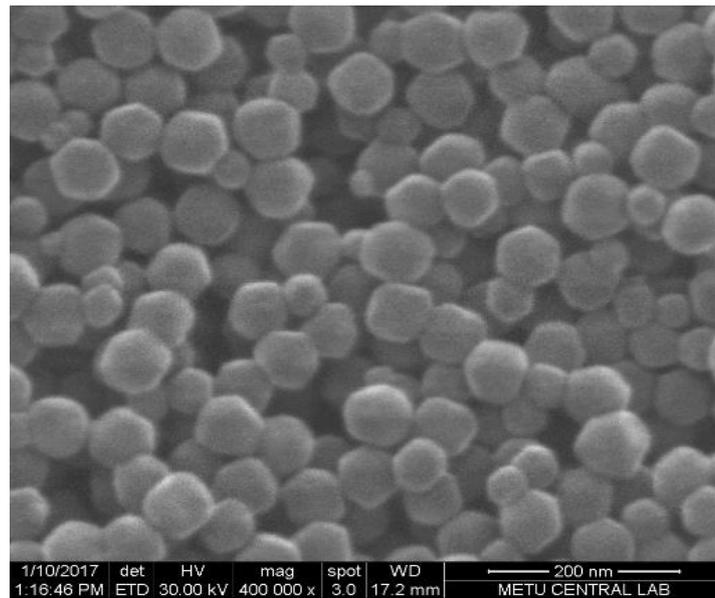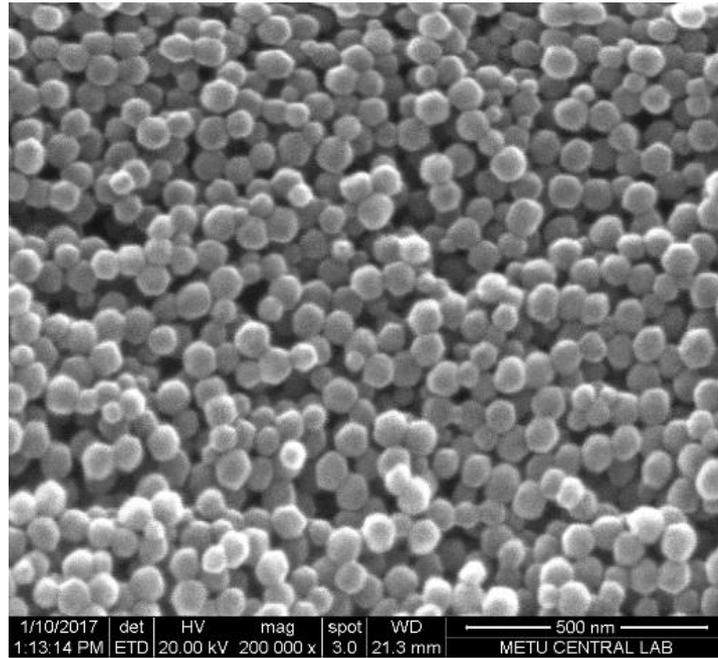
Figure 4.2 The SEM images of the synthesized ZIF-8 crystals

The average particle size of the synthesized ZIF-8 crystals was measured as 79.1 ± 5.0 nm. This particle size value is similar to the particle size of ZIF-8 crystals which was synthesized by Keser et. al. from synthesis solution with 1 Zn^{2+} : 695 MeOH molar ratio [26].

In order to determine the BET surface area and to measure the N_2 adsorption capacity of the synthesized ZIF-8 crystals, N_2 adsorption isotherm was obtained at 77 K (Figure 4.3). According to the analysis, BET surface area of the synthesized ZIF-8 crystals is 1274.8 m^2/g. This value is coherent with the literature. In literature, BET surface area of ZIF-8 powder is nearly equal to 1300 m^2/g [26].
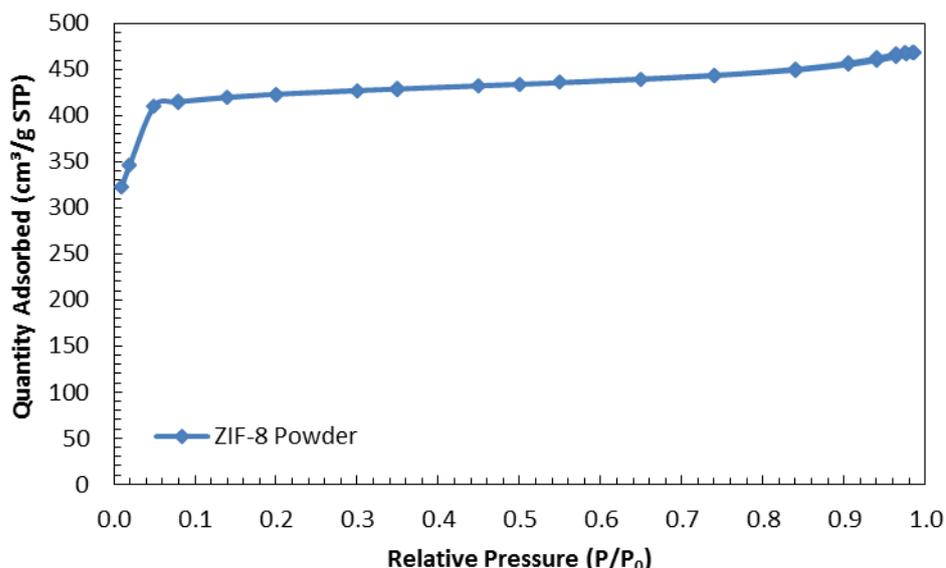
Figure 4.3 Nitrogen adsorption isotherm of ZIF-8 powder at 77 K

4.2. Characterization of Polymer Blend and Mixed Matrix Membranes

Polymer blend and mixed matrix membranes were produced by using water vapor induced phase inversion method. The phase inversion was initiated by exposing the membrane surface to infrared light for different periods of time, and completed by phase inversion was carried out in air with a relative humidity of approximately 80%. Polymer blend membranes were prepared with different blend ratios of PES and PI and mixed matrix membranes were prepared by adding 10 wt.% ZIF-8 to the polymer blends.

There are many parameters which affects the membrane gas permeance and separation performances. Firstly, total membrane and skin layer thickness are the

important parameters for the membrane performance [4]. In this thesis, the thickness of selective skin layer was controlled by infrared light during the phase inversion process. Moreover, the morphological structures of skin layer and support layer give information about the effects of membrane production method on membrane cross-sectional morphology. This means that while the membrane pores have finger like structure due to using liquid water during wet phase inversion, sponge like pores were observed because of using water vapor [16].

The cross-section view of the blend and mixed matrix membranes, which are produced by water vapor during the wet phase inversion and by different ratios, are shown in Figure 4.4.
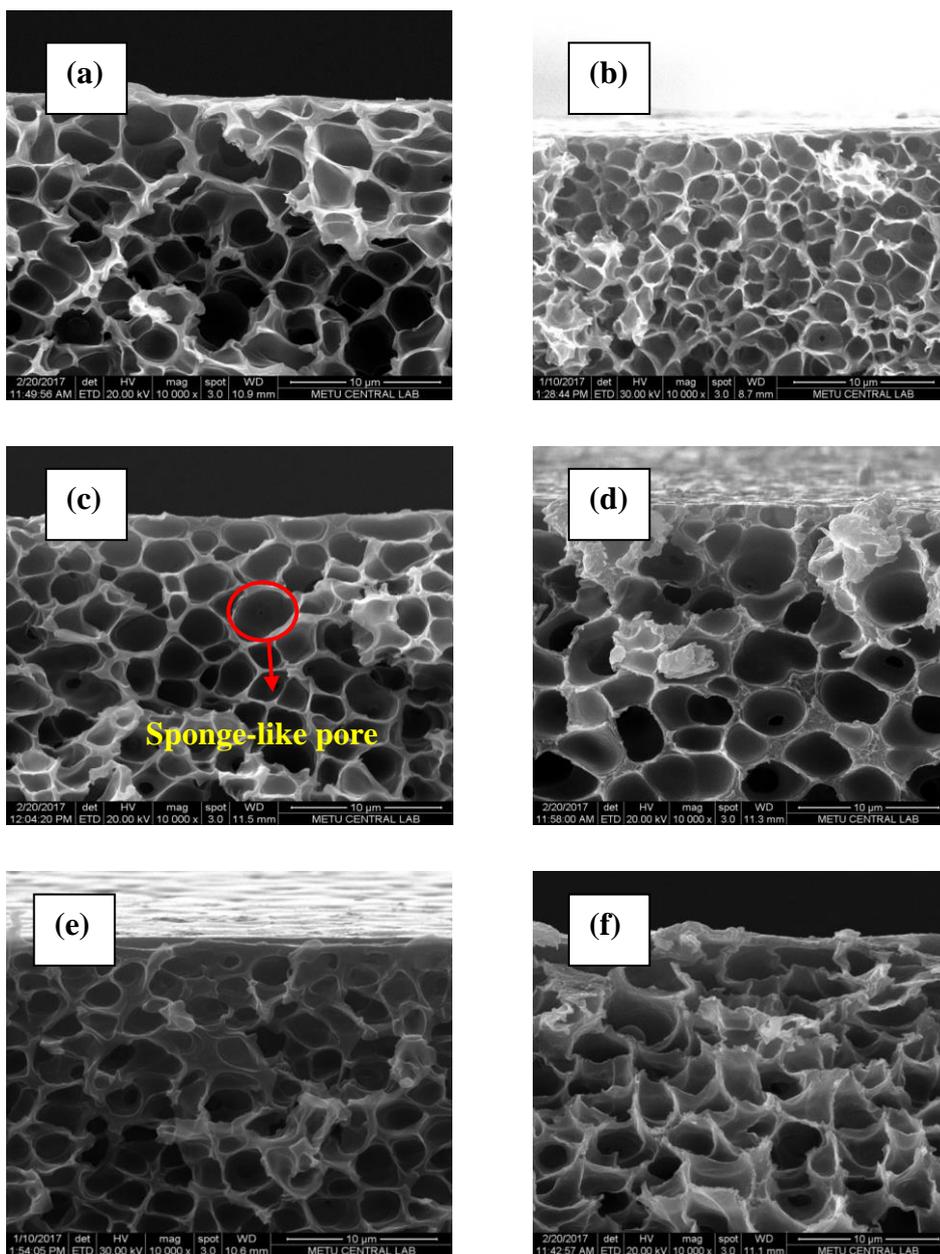
Figure 4.4 (a) PES/PI/20/80, (b) PES/PI/50/50, (c) PES/PI/80/20, (d)
PES/PI/ZIF8/20/80/10, (e) PES/PI/ZIF8/PNA/20/80/0/4,
(f) PES/PI/ZIF8/PNA/20/80/10/4 without IR

According to the SEM images, the membranes, which are produced by water
vapor during the phase inversion, have different pore morphology than the
membrane produced by phase inversion in liquid water. They have sponge-like
pore structure instead of finger-like structure in cross-section for each membrane
composition. When the amount of PES increased in the blend membrane

composition, pore size of the membrane decreased. The calculated avarage pore sizes of the blend membranes are given in Table 4.2:

Table 4.2 The avarage pore sizes of produced blend membranes

Membrane Type	Avarage Pore Size (µm)
PES/PI/20/80	2.7 ± 0.5
PES/PI/50/50	2.1 ± 0.2
PES/PI/80/20	2.0 ± 0.2

In order to prevent ZIF-8 agglomeration and obtain their good dispersion throughout the cross-section of the membrane, the membrane solutions were ultrasonicated longer and ZIF-8 addition to the solution was performed by priming. This procedure helped to prevent agglomeration and provide the good dispersion of ZIF-8 crystals in the membrane matrix. ZIF-8 crystals dispersed throughout the membrane cross-section is shown in Figure 4.5:
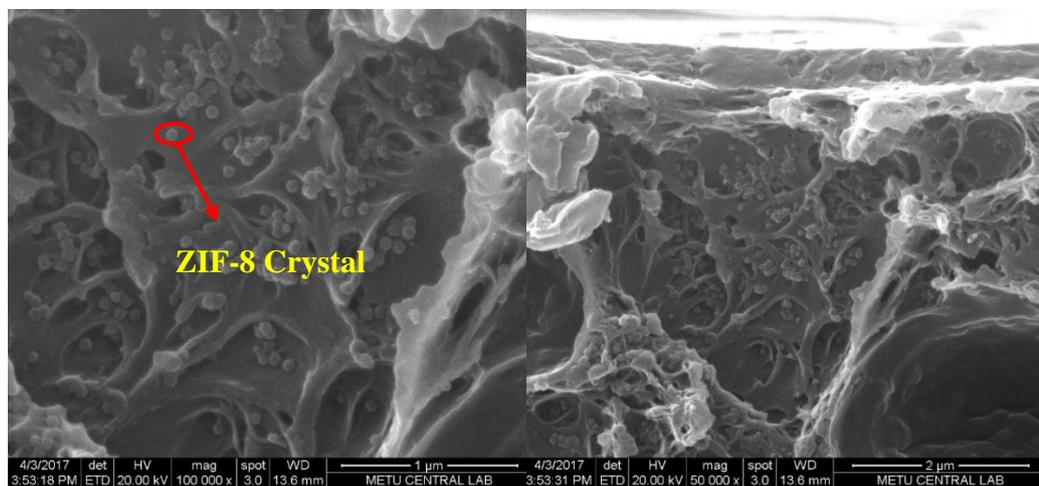
Figure 4.5 Good dispersion of ZIF-8 crystals throughout the membrane cross-section

As seen in Figure 4.5, the homogenously dispersion of ZIF-8 crystals can be easily observed. Moreover, ZIF-8 crystals generally placed at the bottom of

selective skin layer of the membrane. This is the expected situation because of the phase inversion method.

Thermal gravimetric analysis was performed for the produced blend and mixed matrix membranes in order to determine the thermal stability of membrane and the amount of remaining solvent in the membrane pores. In this method, the membrane sample was heated up to 650 °C at a constant 10°C/min heating rate under N_2 atmosphere and the weight loss due to temperature is calculated.

According to TGA results, it can be said that the major weight loss started after 450 °C for all of the tested membranes and this result is parallel with the results in literature [17]. Moreover, when the amount of PES in the membrane composition increases, weight loss of membrane due to temperature increases. This states that PES is less thermally durable than PI [5].

Moreover, the decomposition temperatures of pure PI, PES/PI/20/80, PES/PI/50/50 and PES/PI/80/20 membranes were compared and this comparison were given in Figure 4.6. The decomposition temperature of the membrane means the starting point of the weight loss of the membrane with increasing temperature.
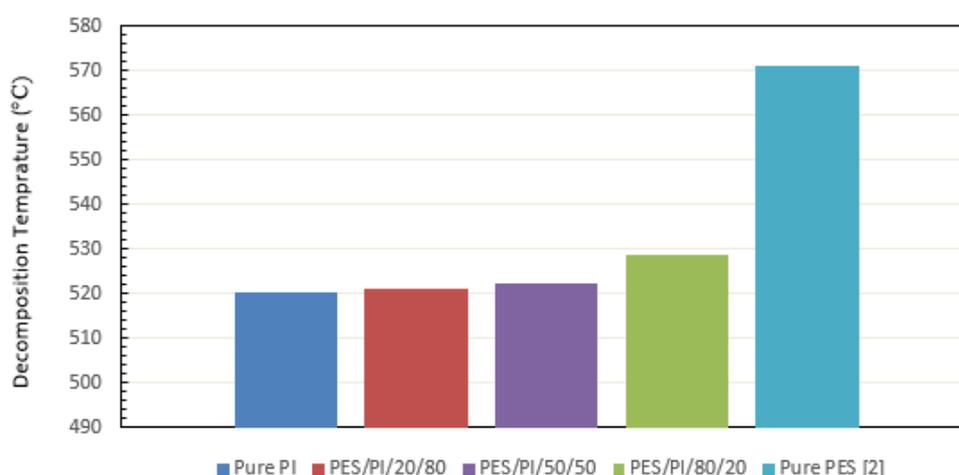
Figure 4.6 Decomposition temperatures of Pure PI, PES/PI/20/80, PES/PI/50/50, PES/PI/80/20 and pure PES [2] membranes

According to Figure 4.6, it is proven that PES is the more thermally durable material than PI again because the decomposition temperatures of membranes increased with increasing the amount of PES into the membrane composition [5]. In order to analyze thermal behavior of the produced mixed matrix membranes, the TGA curves of PES/PI/20/80 and PES/PI/ZIF-8/20/80/10 membranes were plotted in Figure 4.7.
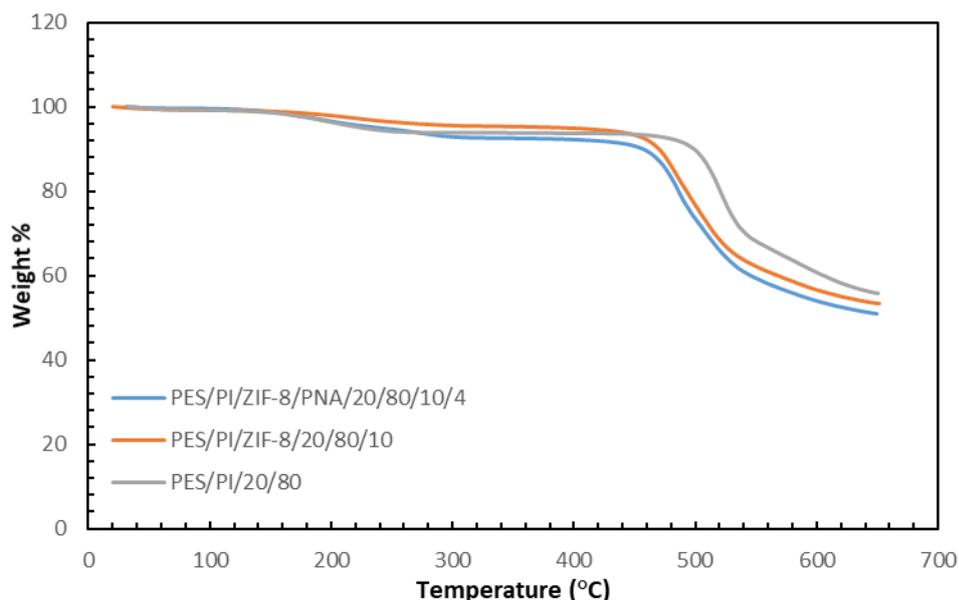
Figure 4.7 TGA curves of PES/PI/20/80, PES/PI/ZIF-8/20/80/10 and PES/PI/ZIF-8/PNA/20/80/10/4 membranes in N_2

According to the TGA curves in Figure 4.7, when ZIF-8 was added to the membrane composition, weight loss of the membranes were almost the same. ZIF-8 addition to the membrane composition may cause a slight decrease in the percentage of residual solid because of thermal decomposition of ZIF-8 [5].

The effect of compatibilizer (pNA) on the thermal behavior of the membranes is also analyzed. For this purpose, PES/PI/ZIF-8/20/80/10 and PES/PI/ZIF-8/PNA/20/80/10/4 membranes were compared by TGA analysis. In Figure 4.7, TGA curves of these membranes were also given. According to the results, pNA has no substantial effect on the thermal behavior of the membrane.

The decomposition temperatures of the same membranes were also compared. The results show that the addition of 4 wt.% compatibilizer to the membrane composition does not significantly affected to the decomposition temperature of the mixed matrix membrane.

In order to determine the glass transition temperatures of the produced blend and mixed matrix membranes, differential scanning calorimetry was used as the analysis method. DSC analysis was carried out for different types of membranes with different polymer ratios and their glass transition temperatures were measured. The measured values were compared with each other (Table 4.3).

Table 4.3 DSC results of the produced blend and mixed matrix membranes

Membrane Type	Glass Transition Temperatures (°C)
PES/PI/20/80	119
PES/PI/50/50	121
PES/PI/80/20	130
PES/PI/ZIF-8/20/80/10	128

DSC analysis results showed that the glass transition temperatures of the PES/PI/20/80 membranes increased with addition of ZIF-8 crystals to the membrane polymer matrix. Moreover, the glass transition temperature of PES/PI/20/80/10 membrane was higher than that of blend membranes.

4.3. Single Gas Permeation through Blend and Mixed Matrix Membranes

In the study, blend and mixed matrix membranes were produced for biogas purification and thus, they were characterized by measuring single gas permeabilities and separating gas mixtures. In the biogas, the volume percentages of CO_2 and CH_4 are higher than the other gases. Therefore, the measurements were performed only for CO_2 and CH_4. Besides, H_2 permeation were also measured as it is non-condensable gas with a small kinetic diameter.

The measurements were carried out at 35°C and 3 bar transmembrane pressure. All membranes, which were tested for the single gas permeance, were produced by dry/wet phase inversion method in air with a relative humidity of 80%. According to the results, it is seen that the membranes which have high selectivity were produced but reproducibility problem, especially for the permeance values, occurs for the produced membranes. The reason of this situation can be related with membrane casting procedure or whether completion of phase inversion of the membrane. Single gas permeation results of all the produced blend and mixed matrix mambranes were given in Appendix B.

4.3.1. Single Gas Permeation Results for Blend Membranes

In order to determine the effect of IR time on the selectivity of blend membrane, the membranes were produced with the same polymer blending ratio. The average permeance and selectivity values and their standard deviations were calculated. Standart deviations of permeances and selectivities were calculated by using measurement results of different membrane pieces. These values of PES/PI/20/80 membrane were tabulated in Table 4.4.

Table 4.4 Permeability and Selectivity Values of PES/PI/20/80 membrane for different IR times

Membrane Type	Permeance (GPU)			Ideal Selectivity		
	H_2	CO_2	CH_4	H_2/CO_2	CO_2/CH_4	H_2/CH_4
PES/PI/20/80 (IR: 0 sec.)	5.42±0.85	1.86±0.32	0.07±0.01	2.9±0.4	26.8±1.09	79.2±14.8
PES/PI/20/80 (IR: 40 sec.)	4.40±0.00	2.28±0.00	0.09±0.00	1.9±0.0	25.3±0.0	48.9±0.0
PES/PI/20/80 (IR: 80 sec.)	3.28±0.05	1.20±0.03	0.05±0.00	2.7±0.04	24.0±0.7	65.7±1.1
PES/PI/20/80 (IR: 120 sec.)	0.55±0.00	0.38±0.00	0.02±0.00	1.5±0.0	19.7±0.0	28.9±0.0

When the IR exposing time was extended during the phase inversion, permeances of PES/PI/20/80 membranes decreased. Similarly, H_2/CO_2, H_2/CH_4 and CO_2/CH_4 selectivities decreased with increasing IR exposing period from 80 sec. to 120

sec. during the dry phase inversion. The graphical representation of this results were given in Figure 4.8:
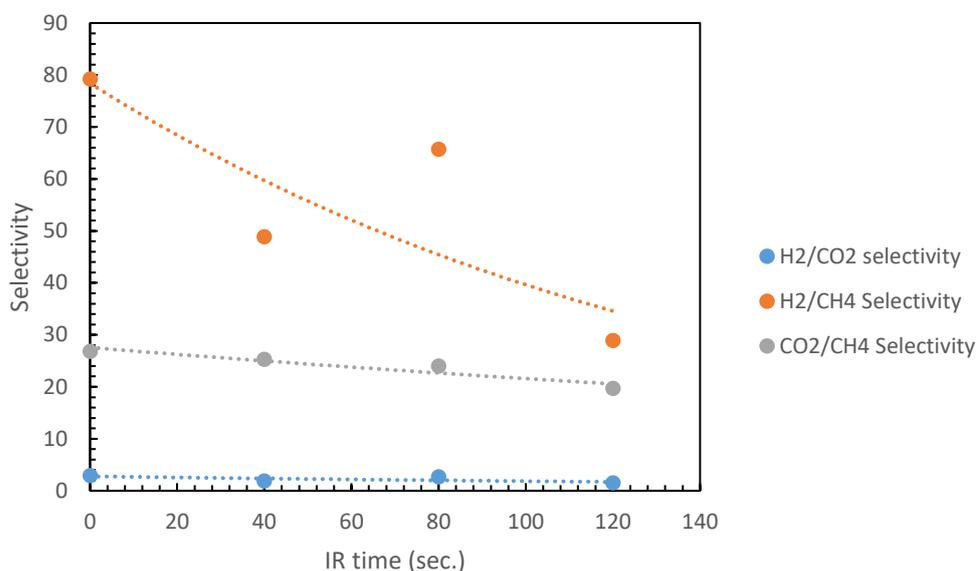
Figure 4.8 Selectivity vs IR time graph for PES/PI/20/80 membrane

In order to observe the effect of PI content on the permeance and selectivity, the blend membranes with different PI content were produced with 120 sec IR period. The permeance and selectivity values of these membranes were given in Table 4.5:

Table 4.5 The permeance and selectivity values of blend membranes which are produced with 120 sec. IR and chosen for the comparison

Membrane Type	Permeance (GPU)			Ideal Selectivity		
	H_2	CO_2	CH_4	H_2/CO_2	CO_2/CH_4	H_2/CH_4
PES/PI/20/80	0.55	0.38	0.02	1.5	19.7	28.9
PES/PI/50/50	1.74	0.90	0.09	1.9	10.0	19.3
PES/PI/80/20	5.37	2.08	0.09	2.6	23.1	59.7

The effect of PI amount into the membrane composition on H_2 permeance were given in Figure 4.9. When the amount of PI increases in the membrane composition, all permeance of the membrane decreases.

42
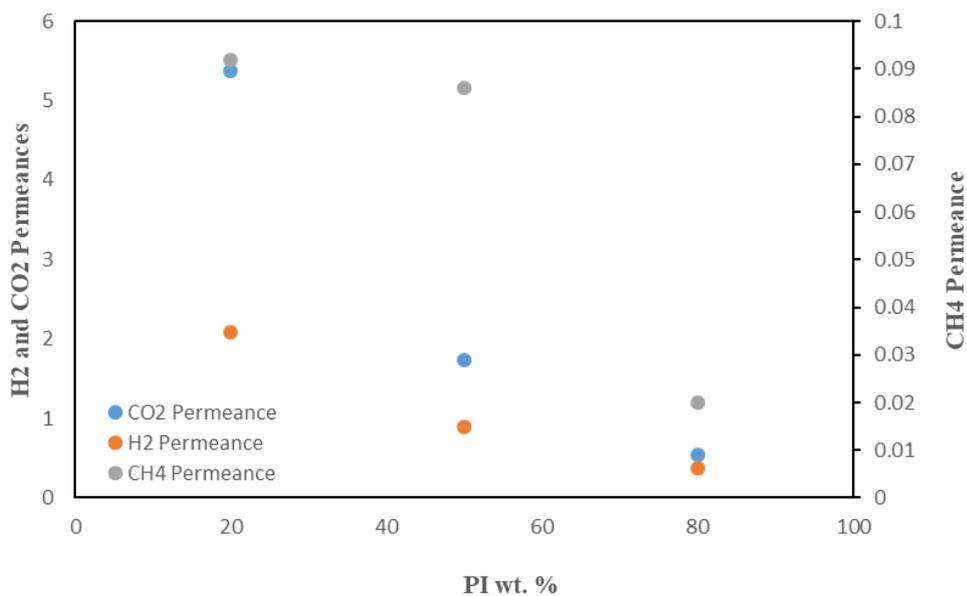
Figure 4.9 H_2, CO_2 and CH_4 permeances vs PI wt.% graph for the produced blend membrane with 120 sec. IR lamb

While the highest gas permeance was achieved for H_2 gases, the lowest one was obtained for CH_4 gases. This situation was the expected result because of the kinetic diameters of H_2, CO_2 and CH_4 gas molecules. Moreover, all permeances decreases with increasing PI amount of the produced membrane compositions.

After the comparison of H_2, CO_2 and CH_4 permeances of the membranes with different blend ratios, H_2/CO_2, CO_2/CH_4 ve H_2/CH_4 ideal selectivities of the same membranes were also evaluated by graphical approach. The effect of PI amount on H_2/CO_2, CO_2/CH_4 and H_2/CH_4 selectivities of the membrane is given in Figure 4.10.
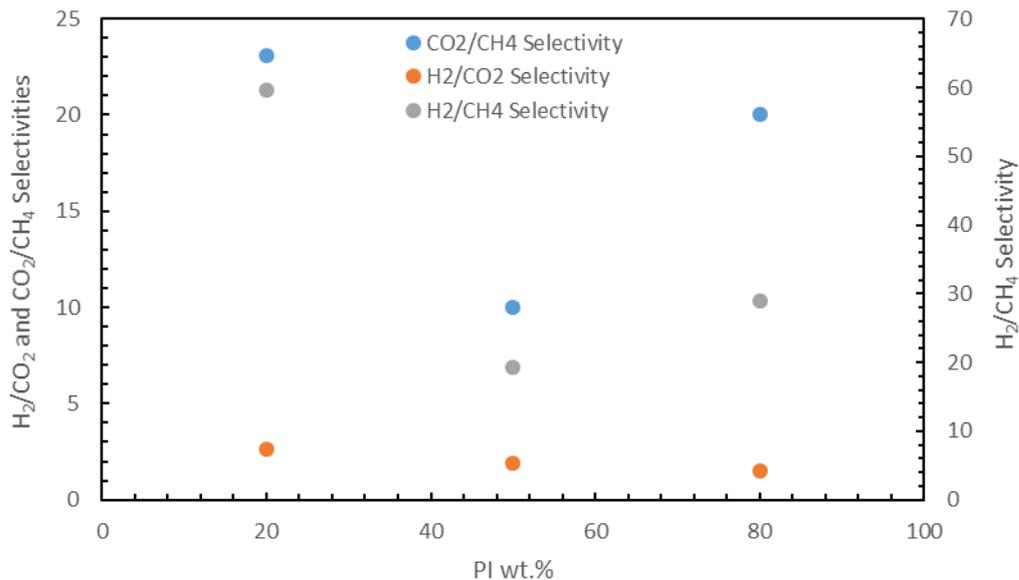
Figure 4.10 H_2/CO_2, CO_2/CH_4 and H_2/CH_4 selectivities vs PI wt.% graph for blend membranes with 120 sec. IR lamb

As seen in Figure 4.10, when the amount of PI increased into the membrane composition, H_2/CO_2 selectivity decreased like permeance values.

The change of CO_2/CH_4 selectivity of the produced membranes with increasing PI is also investigated. It was observed that when the amount of PI increased from 20 wt.% to 50 wt.%, CO_2/CH_4 selectivity decreased but the PI amount increased to the 80 wt.%, selectivity value increased.

Finally, the change of H_2/CH_4 selectivity because of changing the PI amount is observed. The results are similar with the CO_2/CH_4 selectivity analysis, that is, H_2/CH_4 selectivity first decreased and then increased with increasing PI wt.%.

When the PI amount increased into the membrane composition, it is expected that the selectivities slightly decreased. Because of the reproducibility problem of membrane solutions, it was not observed for H_2/CH_4 and CO_2/CH_4 selectivities of the membranes.

4.3.2. Single Gas Permeation Results for Mixed Matrix Membranes

The single gas permeances through mixed matrix membranes with 10 wt. % ZIF-8 was performed. For this analysis, PES/PI/ZIF8/20/80/10 and PES/PI/ZIF8/80/20/10 membranes were used. Firstly, the effect of IR time on the mixed matrix membrane performance was analyzed. For this purpose, average permeances of the different produced membranes, selectivity and their standard deviation values of PES/PI/ZIF-8/20/80/10 membrane were calculated. These calculated data were given in Table 4.6. Because of that one piece of PES/PI/ZIF-8/20/80/10 without IR time was produced, standart deviation of this was shown as zero.

Table 4.6 Permeability and Selectivity Values of PES/PI/ZIF-8/20/80/10 membrane for different IR times

Membrane Type	Permeance (GPU)			Ideal Selectivity		
	H_2	CO_2	CH_4	H_2/CO_2	CO_2/CH_4	H_2/CH_4
PES/PI/ZIF8/ 20/80/10 (IR: 0 sec.)	14.22±0.00	5.26±0.00	0.40±0.00	2.7±0.0	13.2±0.0	35.6±0.0
PES/PI/ZIF8/ 20/80/10 (IR: 40 sec.)	4.78±1.53	2.32±0.20	0.09±0.005	2.0±0.5	27.1±0.9	55.3±14.7
PES/PI/ZIF8/ 20/80/10 (IR: 80 sec.)	5.15±0.44	1.90±0.16	0.08±0.01	2.7±0.0	24.4±0.6	66.1±1.2
PES/PI/ZIF8/ 20/80/10 (IR: 120 sec.)	1.83±0.02	0.79±0.02	0.04±0.005	2.4±0.05	22.9±2.9	53.2±7.2

By using the results in Figure 4.6, it can be said that when the PES/PI/ZIF-8/20/80/10 mixed matrix membrane was produced firstly without IR light and then with 40 sec. IR light, the CO_2/CH_4 selectivity of the membrane sharply increased. However, when the IR time increased from 40 sec. to 80 and 120 sec., the CO_2/CH_4 selectivity values of the PES/PI/ZIF-8/20/80/10 mixed matrix membrane slightly decreased. The graphical representation of this was given in Figure 4.11.
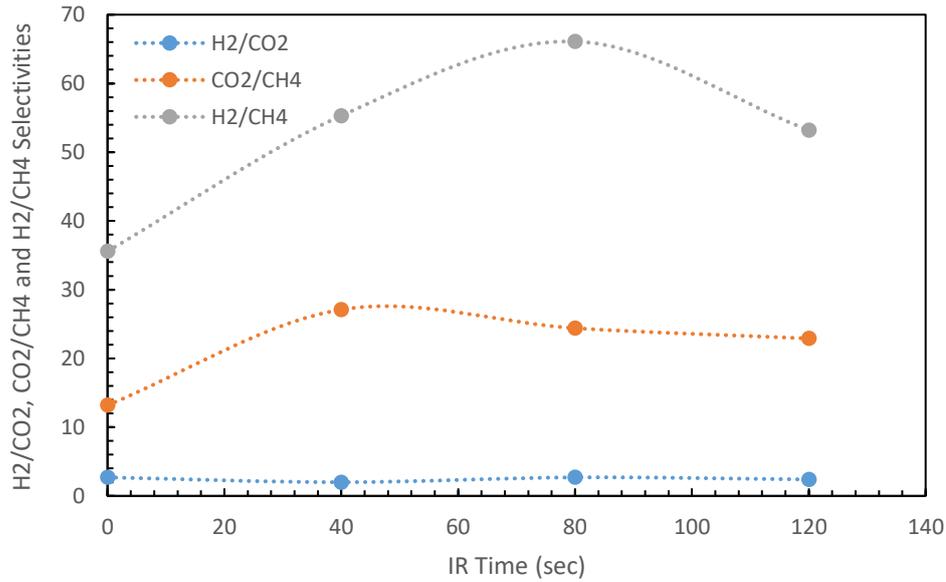
Figure 4.11 H_2/CO_2, CO_2/CH_4 and H_2/CH_4 selectivities vs IR time graph for PES/PI/ZIF-8/20/80/10 mixed matrix membrane

For the comparison of blend and mixed matrix membranes, PES/PI/20/80, PES/PI/50/50, PES/PI/ZIF-8/20/80/10 and PES/PI/ZIF-8/80/20/10 membranes produced by 40 sec. IR time were chosen. The single gas permeances and ideal selectivities of the chosen blend and mixed matrix membranes were tabulated in Table 4.7.

Table 4.7 Single Gas Permeances and Ideal Selectivities of the chosen blend and mixed matrix membranes for the comparison (IR time: 40 sec)

Membrane Type	Permeance (GPU)			Ideal Selectivity		
	H_2	CO_2	CH_4	H_2/CO_2	CO_2/CH_4	H_2/CH_4
PES/PI/20/80	4.40	2.28	0.09	1.9	25.3	48.9
PES/PI/ZIF-8/ 20/80/10	4.78	2.32	0.09	2.0	27.1	55.3
PES/PI/ZIF-8/ 80/20/10	5.18	2.05	0.07	2.5	29.3	74.0

According to the results, the mixed matrix membranes have higher H_2/CO_2 ideal selectivities than blend membranes as expected. On the other hand, the addition of ZIF-8 crystals into the membrane composition does not have crucial effect for H_2 gas permeance contrary to expectations. The reason of this situation can be related with the ZIF-8 agglomeration in the polymer matrix as observing the SEM images.

4.4. Mixed Gas Separation Results for Blend and Mixed Matrix Membranes

After the single gas permeation and ideal selectivity analysis for the produced blend and mixed matrix membranes was completed, mixed gas separation performance tests were performed. For this purpose, the used membranes and their content were tabulated in Table 4.8. These membranes were produced by exposing to infrared light and water vapor with 80% RH in a glove box during the water vapor induced phase inversion.

Table 4.8 The composition of the membranes used for mixed gas separation tests

Membrane Code	Membrane Name	PES wt.%	PI wt.%	ZIF-8 wt.%	pNA wt%	IR time (sec.)
M1	PES/PI/20/80	20	80	-	-	0
M2	PES/PI/20/80	20	80	-	-	80
M3	PES/PI/ZIF-8 20/80/10	20	80	10	-	0
M4	PES/PI/ZIF-8 20/80/10	20	80	10	-	40
M5	PES/PI/ZIF-8 20/80/10	20	80	10	-	80
M6	PES/PI/ZIF-8/pNA 20/80/10/4	20	80	10	4	40

All of the membranes given in Table 4.8 were tested in order to determine CO_2 and CH_4 single gas permeance and CO_2/CH_4 gas mixture separation. After that, ideal selectivities and separation factors of these membranes were calculated. For

47

all these membranes, CO_2 and CH_4 gas permeance and selectivity data were given in Appendix C.

4.4.1 Temperature and Feed Gas Composition Effects on Gas Separation Performances of Blend and Mixed Matrix Membranes

In order to understand the effect of temperature and feed gas composition on gas separation performances of blend and mixed matrix membranes, the membranes were tested with different CO_2/CH_4 feed gas composition at different temperatures. For the comparison, M1 and M3 membranes were chosen as blend and mixed matrix membranes, respectively, and their permeance and CO_2/CH_4 selectivity results were given. Permeance versus temperature graph for M1 membrane was shown in Figure 4.12.
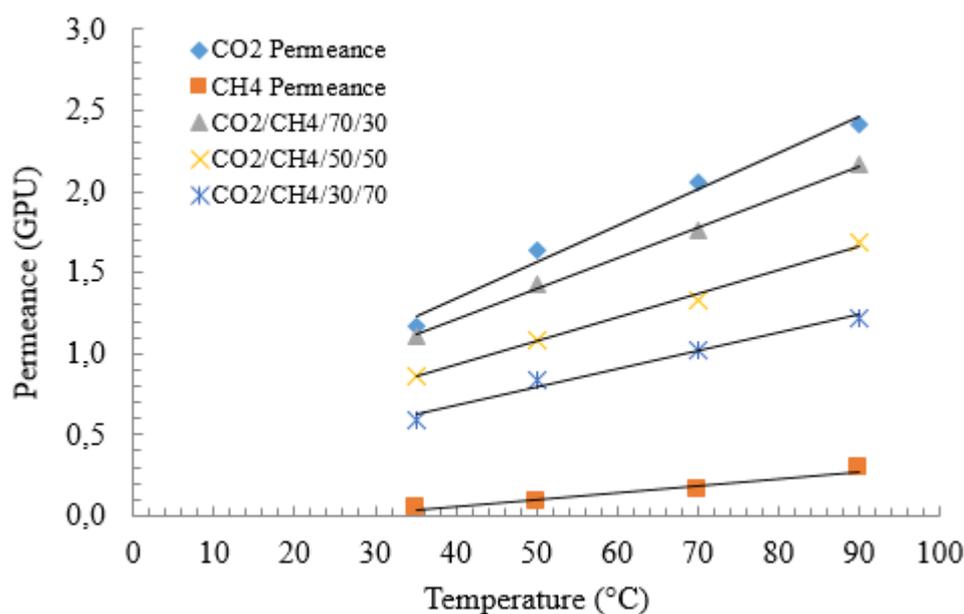
Figure 4.12 Permeance versus temprature graph of M1 membrane with different feed gas compositions

When the permeance vs temperature graph of M1 membrane was examined, it was seen that permeances linearly increased with temperature. Moreover, when the amount of CO_2 in the feed gas composition decreased, the M1 membrane permeances also decreased.

48

CO_2/CH_4 selectivity versus temperature graph of M1 membrane was shown in Figure 4.13.
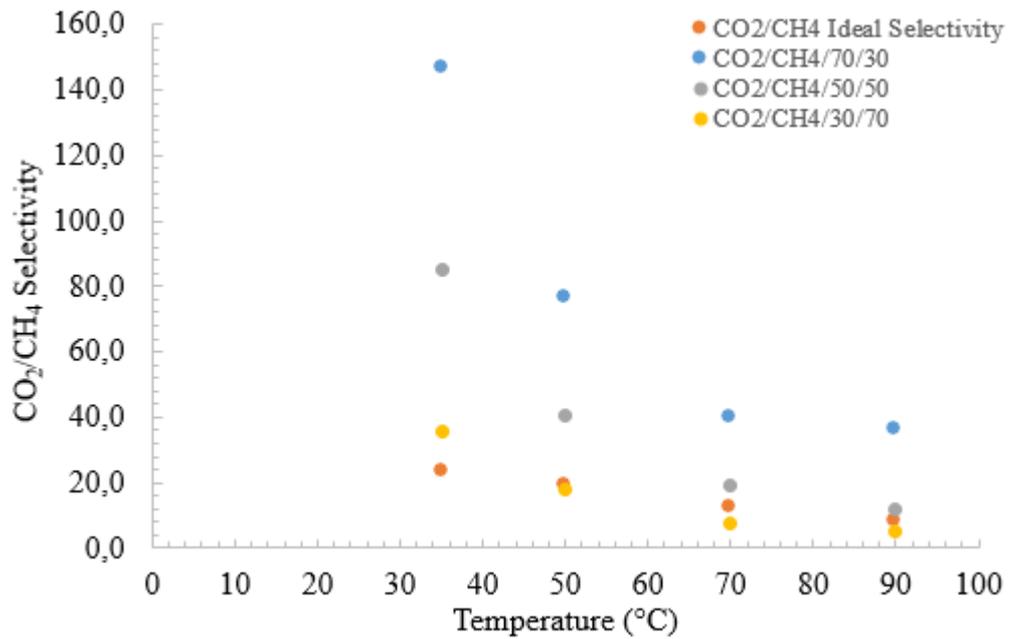
Figure 4.13 CO_2/CH_4 selectivity versus temperature graph of M1 membrane with different feed gas compositions

According to Figure 4.13, the highest CO_2/CH_4 selectivity value was 146.93 at 35°C and CO_2/CH_4/70/30 feed composition. This value decreased with increasing temperature or increasing the amount of CH_4 in the feed gas. On the other hand, the lowest CO_2/CH_4 selectivity was obtained as 5.27 at 90°C and CO_2/CH_4/30/70 feed composition. Moreover, it can be said that ideal selectivity of M1 membrane showed a linear trend compared to the mixed gas selectivity trends and it decreased from 23.33 to 8.38 with increasing temperature.

CO_2% and CH_4% in permeate of M1 membrane were measured for the different feed gas compositions at different temperatures. CO_2% in permeate vs. T and CH_4% in permeate vs. T graphs at different feed gas compositions were represented in Figure 4.14 and Figure 4.15.
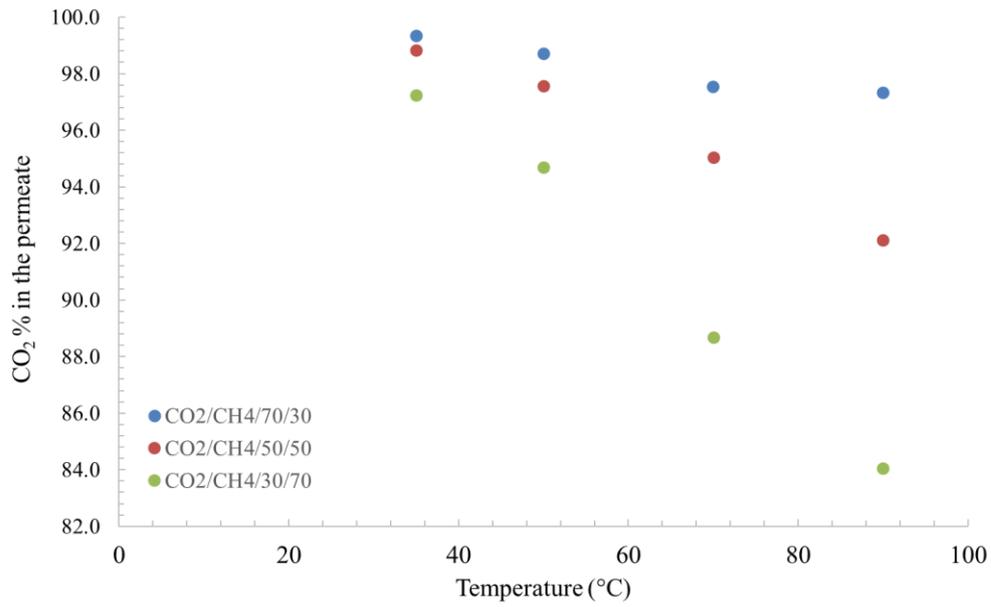
Figure 4.14 CO$_2$% in the permeate vs. temperature graph of M1 membrane for different feed gas compositions
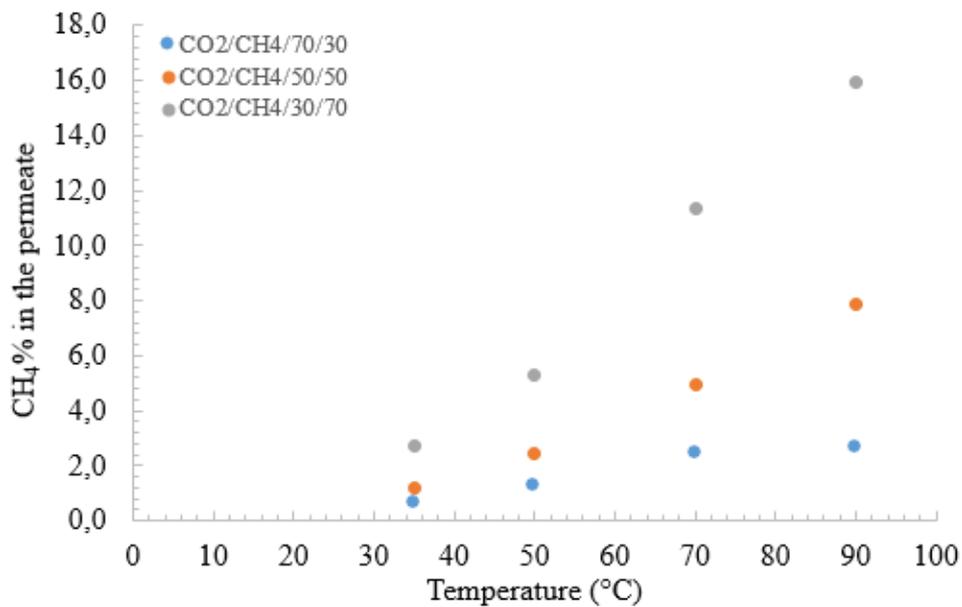
Figure 4.15 CH$_4$% in the permeate vs temerature graph of M1 membrane for different feed gas compositions

It is observed that while CO_2% in permeate decreased with increasing temperature, CH_4% in permeate increased. Also, the decreasing the amount of CO_2 into the feed gas compositions gave the same results. That is, the highest percentage of CO_2 in permeate was achieved at $CO_2/CH_4/70/30$ feed gas composition. While the CO_2% in permeate slightly decreased during the $CO_2/CH_4/70/30$ feed gas composition, it decreased faster during the $CO_2/CH_4/30/70$ feed gas composition and the opposite case was seen for CH_4% in permeate.

M3 membrane was also used in order to observe the effect of temperature and feed gas composition on the gas separation performance of PES/PI/ZIF-8 mixed matrix membrane. For this purpose, permeance and temperature graph of M3 membrane was given in Figure 4.16.
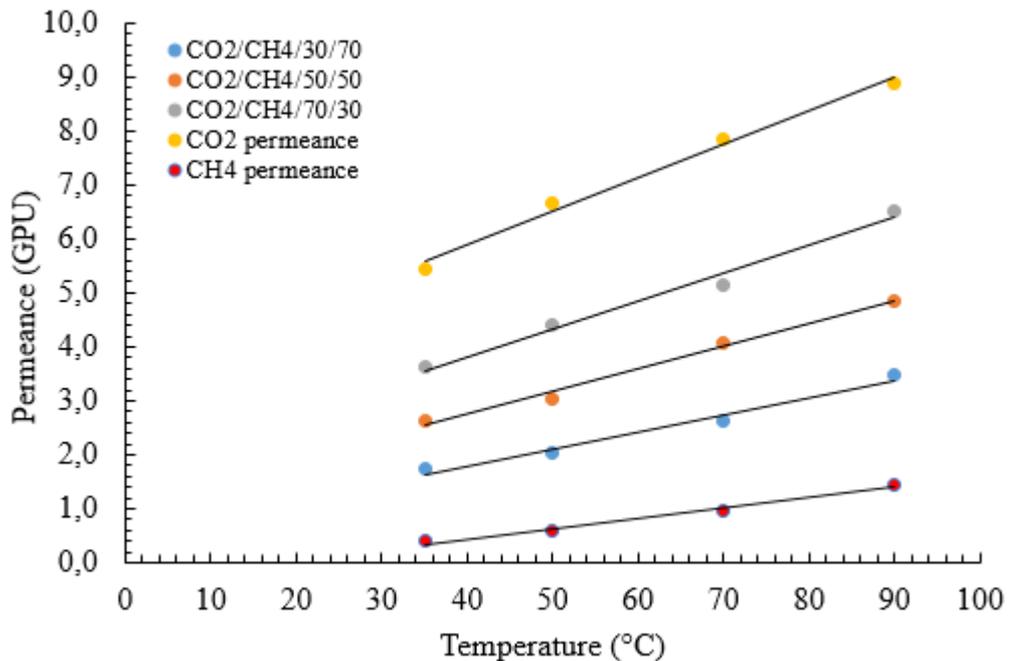

Figure 4.16 Permeance versus Temperature graph of M3 membrane with different feed gas compositions

When the permeance vs temperature graph of M3 membranes in Figure 4.16 was analyzed, the linear trend for permeance values of M3 membrane was observed like M1 membrane and all permeance values increased with increasing

temperature. The CO_2 and CH_4 permeances of M3 membranes were in the range of 5.43 – 8.88 GPU and 0.39 – 1.44 GPU, respectively. The permeances at the other feed gas compositions were placed between pure CO_2 and CH_4 permeance values as expected. At the same temperature, permeance value increased with increasing the amount of CO_2 in the feed gas.

The CO_2/CH_4 selectivities of M3 membrane were calculated by using the permeance values and CO_2/CH_4 selectivities versus temperature graph was plotted in order to investigate the effect of temperature and feed gas composition on mixed matrix membrane selectivity. CO_2/CH_4 selectivity versus temperature graph of M3 membrane was shown in Figure 4.17.
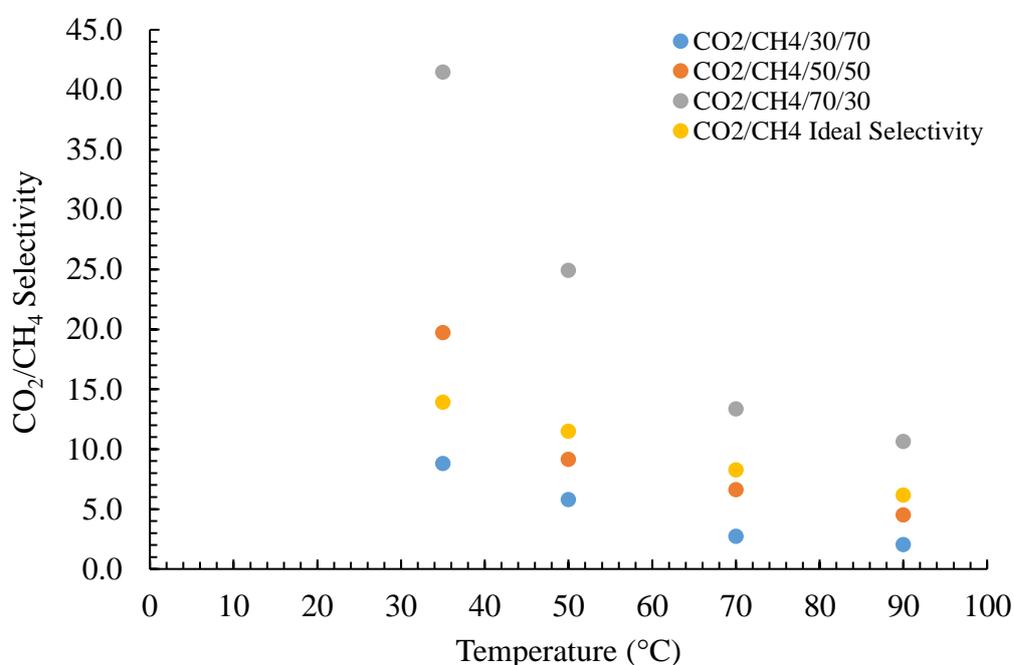

Figure 4.17 CO_2/CH_4 selectivity versus temperature graph at different feed gas compositions

According to the Figure 4.17, the trend of CO_2/CH_4 selectivity were nearly the same as M1 membrane throughout temperature rise and different feed gas composition. The highest selectivity value was achieved as 41.46 at 35°C and $CO_2/CH_4/70/30$ feed gas composition and the lowest one was obtained as 2.03 at 90°C and $CO_2/CH_4/30/70$ feed gas composition. At the same temperature, CO_2/CH_4 selectivities increased with increasing the amount of CO_2 in the feed

gas. On the other hand, selectivity values decreased with increasing temperature at the same feed gas composition. When the temperature increased, the ideal selectivity decreased from 13.92 to 6.17.

CO_2% and CH_4% in permeate of M3 membrane were measured for the different feed gas compositions at different temperatures. CO_2% in permeate vs. temperature and CH_4% in permeate vs. temperature graphs at different feed gas compositions were represented in Figure 4.18 and Figure 4.19.
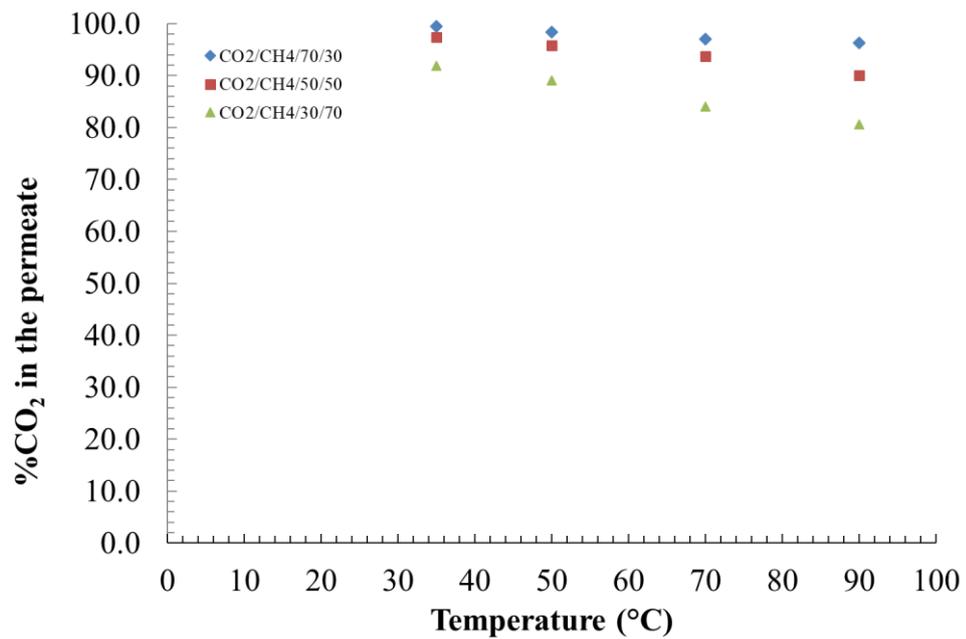

Figure 4.18 CO_2% in the permeate vs. temperature graph of M3 membrane for different feed gas compositions
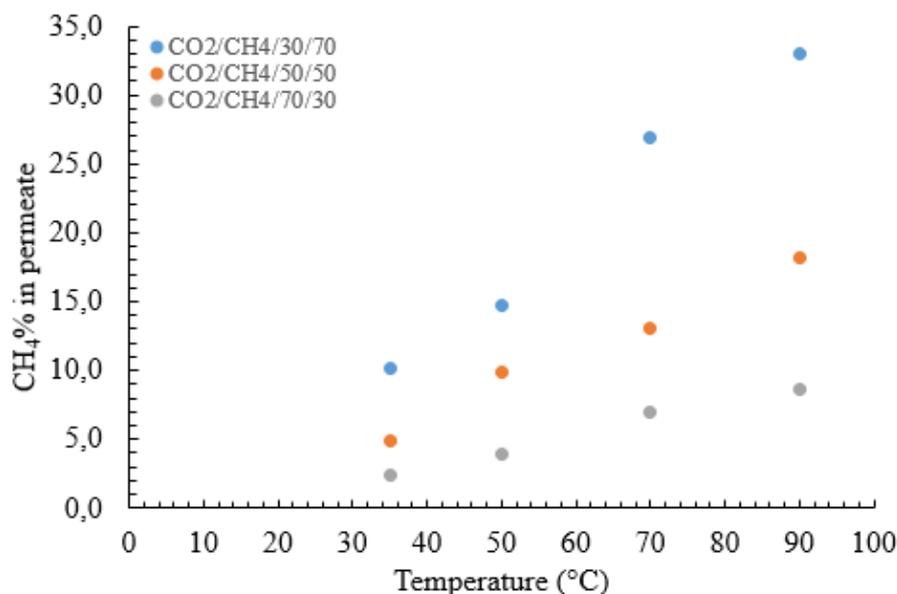
Figure 4.19 CH$_4$% in the permeate vs. temperature graph of M3 membrane for different feed gas compositions

When Figure 4.18 and Figure 4.19 were analyzed, it was seen that the CO$_2$% and CH$_4$% in permeate graphs have the same trend with the M1 membrane. The highest percentage of CO$_2$ in permeate was achieved as 97.6% at 35°C and CO$_2$/CH$_4$/70/30 feed gas composition and the highest percentage of CH$_4$ in permeate was obtained as 32.9% at 90°C and CO$_2$/CH$_4$/30/70 feed gas composition.

The trends of blend and mixed matrix membrane for mixed gas separation were very similar. For both of the membranes, permeances increased and selectivities decreased with increasing temperature. It is related with the change of membrane pore size with different temperature value. Moreover, when the amount of CO$_2$ increased in feed gas composition, permeances and selectivities also increased due to the competitive adsorption between CO$_2$ and CH$_4$ gas molecules.

4.4.2 IR Time Effects on Gas Separation Performances of Blend and Mixed Matrix Membranes

During the membrane preparation, dry phase inversion was performed by using IR light in order to form selective skin layer on the top of the membrane. The

thickness of this skin layer can be adjusted by changing the IR time during the dry phase inversion. The blend and mixed matrix membranes which are produced by using different IR time were analyzed in order to determine the IR time effect on membrane gas separation performance. For this purpose, the blend membranes produced by 0 sec. and 80 sec.IR time were firstly compared in terms of their permeances and CO_2/CH_4 selectivities. The permeance values of blend membranes depending on IR time were given in Table 4.9.

Table 4.9 IR time effect on permeance of PES/PI/20/80 blend membrane at different feed gas composition (T=35°C)

Membrane Code: PES/PI/20/80		
Feed Gas Comp.	Permeance (GPU)	
	IR time: 0 sec. (M1)	IR time: 80 sec. (M2)
Pure CO_2	1.17	0.86
$CO_2/CH_4/70/30$	1.11	0.63
$CO_2/CH_4/50/50$	0.87	0.48
$CO_2/CH_4/30/70$	0.59	0.35
Pure CH_4	0.05	0.03

According to Table 4.9, it was seen that the permeance values of the produced blend membranes decreased with increasing IR time during the dry phase inversion. This decline was shown for each feed gas composition. This situaition is expected result because the selective skin layer was thicken by increasing IR time and quickly vaporizing solvent during the phase inversion. After the permeance evaluation, CO_2/CH_4 selectivity changes due to different IR time were investigated. For this purpose, CO_2/CH_4 selectivities of the blend membranes depending on IR time were given in Table 4.10.

Table 4.10 IR time effect on CO_2/CH_4 selectivities of PES/PI/20/80 blend membrane at different feed gas composition (T=35°C)

Membrane Code: PES/PI/20/80		
Feed Gas Comp.	**CO_2/CH_4 Selectivity**	
	IR time: 0 sec.	**IR time: 80 sec.**
CO_2/CH_4/70/30	146.93	153.06
CO_2/CH_4/50/50	84.84	50.52
CO_2/CH_4/30/70	35.40	28.50

According to Table 4.10, while the CO_2/CH_4 selectivity increased with slightly increasing IR time for CO_2/CH_4/70/30 feed gas composition, it decreased with increasing IR time for CO_2/CH_4/50/50 and CO_2/CH_4/30/70 feed gas compositions. Moreover, the selectivities decreased with decreasing CO_2 content of the feed. Because of the denser structure of membranes obtained at longer IR times, lower permeances and higher selectivities are expected. However, according to the results, both of permeances and selevities decreased with increasing IR time. This can be resulted with nonproducible selective skin layer of the membranes during the production.

The IR time effect was also investigated on mixed matrix membranes. For this purpose, mixed matrix membranes were produced by using different IR time (0, 40 and 80 sec.) during the dry phase inversion. The produced membranes were tested in order to observe gas separation performance. The permeances of mixed matrix membranes at different feed gas composition were tabulated for different IR time in Table 4.11.

Table 4.11 IR time effect on permeance of PES/PI/ZIF-8/20/80/10 mixed matrix membrane at different feed gas composition (T=35°C)

Membrane Code: PES/PI/ZIF-8/20/80/10			
	Permeance (GPU)		
Feed Gas Comp.	IR time: 0 sec. (M3)	IR time: 40 sec. (M4)	IR time: 80 sec. (M5)
Pure CO_2	5.43	2.79	1.33
$CO_2/CH_4/70/30$	3.61	2.36	1.26
$CO_2/CH_4/50/50$	2.64	1.63	0.91
$CO_2/CH_4/30/70$	1.73	0.95	0.57
Pure CH_4	0.39	0.21	0.07

According to Table 4.11, the permeances of PES/PI/ZIF-8/20/80/10 mixed matrix membranes decreased with extending IR exposure period for each feed gas composition like the blend membranes. It is the expected because the selective skin layer thickness is likely to increase with IR time.

CO_2/CH_4 selectivities of the mixed matrix membranes depending on IR times were given for different feed gas compositions in Table 4.12.

Table 4.12 IR time effect on CO_2/CH_4 selectivities of PES/PI/ZIF-8/20/80/10 mixed matrix membrane at different feed gas composition (T=35°C)

Membrane Code: PES/PI/ZIF-8/20/80/10			
	CO_2/CH_4 Selectivity		
Feed Gas Comp.	IR time: 0 sec. (M3)	IR time: 40 sec. (M4)	IR time: 80 sec. (M5)
$CO_2/CH_4/70/30$	41.46	174.46	98.85
$CO_2/CH_4/50/50$	19.72	37.11	43.38
$CO_2/CH_4/30/70$	8.79	11.39	17.84

According to Table 4.12, the CO_2/CH_4 selectivities of the produced mixed matrix membranes increased with increasing IR time at $CO_2/CH_4/50/50$ and $CO_2/CH_4/30/70$ feed gas compositions. For the $CO_2/CH_4/70/30$ feed gas

compositions, the selectivities increased from 0 sec. to 40 sec. IR time and they decreased when the IR time increased to 80 sec.

4.4.3 Filler Material (ZIF-8) Effects on Gas Separation Performances of Blend and Mixed Matrix Membranes

In this study, mixed matrix membranes were produced by adding filler material (ZIF-8 crystals) to the blend membrane compositions. The aim is to enhance gas separation performances of the membranes provided by ZIF-8 crystals. For this purpose, ZIF-8 crystals are desired to be in selective skin layer during the membrane production. After the preparation of blend and mixed matrix membranes, their permeance and selectivity values were compared with each other.

In Figure 4.20, the comparison of permeances of PES/PI/20/80 blend and PES/PI/ZIF-8/20/80/10 mixed matrix membranes were given. In order to compare filler material effect only, the other variables which are temperature and IR time were kept constant.
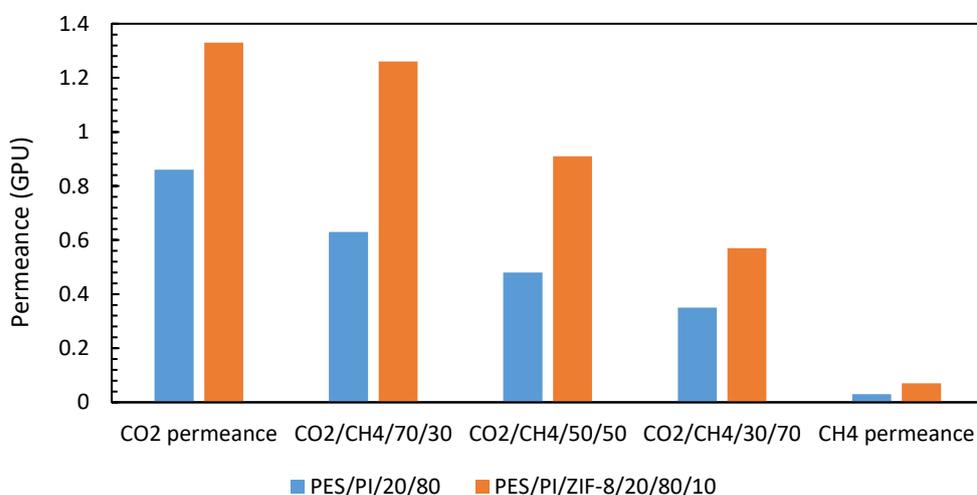
Figure 4.20 Filler material (ZIF-8) effect on permeances of PES/PI/20/80 blend and PES/PI/ZIF-8/20/80/10 mixed matrix membranes (IR time: 80 sec.)

The membranes, which were shown in Figure 4.20, were produced by using 80 sec. IR time. Moreover, the given results belongs to gas separation tests

performed at 35°C. According to Figure 4.21, it was seen that the addition of filler material to the membrane provided higher permeances. This situation can be observed for all types of feed.

The CO_2/CH_4 selectivity of PES/PI/20/80 blend and PES/PI/ZIF-8/20/80/10 mixed matrix membranes were compared in Figure 4.21.
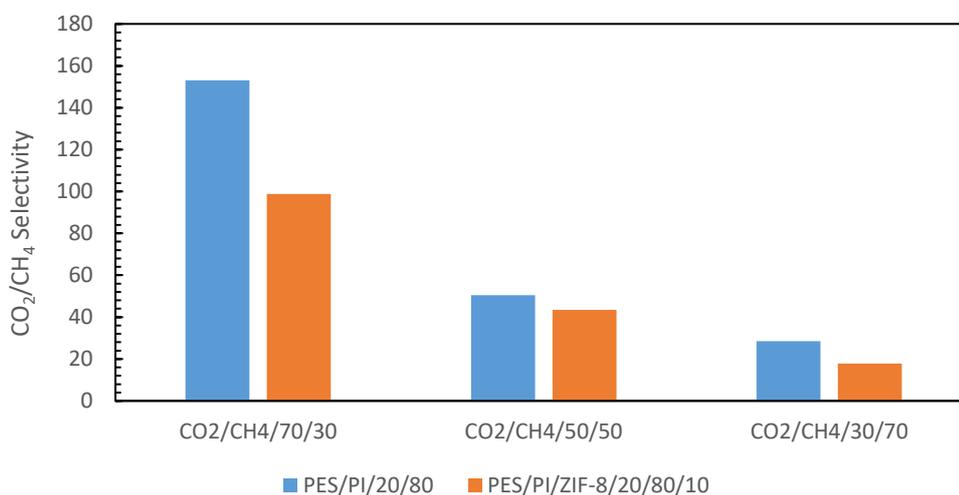
Figure 4.21 Filler material (ZIF-8) effect on CO_2/CH_4 selectivities of PES/PI/20/80 blend and PES/PI/ZIF-8/20/80/10 mixed matrix membranes (IR time: 80 sec.)

When Figure 4.21 was examined, it was observed that the CO_2/CH_4 selectivities of PES/PI/20/80 blend and PES/PI/ZIF-8/20/80/10 mixed matrix membranes decreased with adding filler material to the membrane polymer matrix.

4.4.4 Compatibilizer (pNA) Effects on Gas Separation Performances of Mixed Matrix Membranes

During the mixed matrix membrane preparation, compatibility between polymer and filler may be a critical problem reducing membrane performance. Low compatibility between membrane materials may result in voids formed at the polymer/filler interface. In order to prevent this problem, a compatibilizer can be used during the membrane production. For this purpose, 4 wt.% pNA was added to the produced mixed matrix membranes and these membranes were tested for

determination of their gas separation performances. Then, the results were compared with the mixed matrix membrane which was produced without pNA.

The comparison of permeances of PES/PI/ZIF-8/20/80/10 mixed matrix and PES/PI/ZIF-8/pNA/20/80/10/4 membranes were given in Figure 4.22.
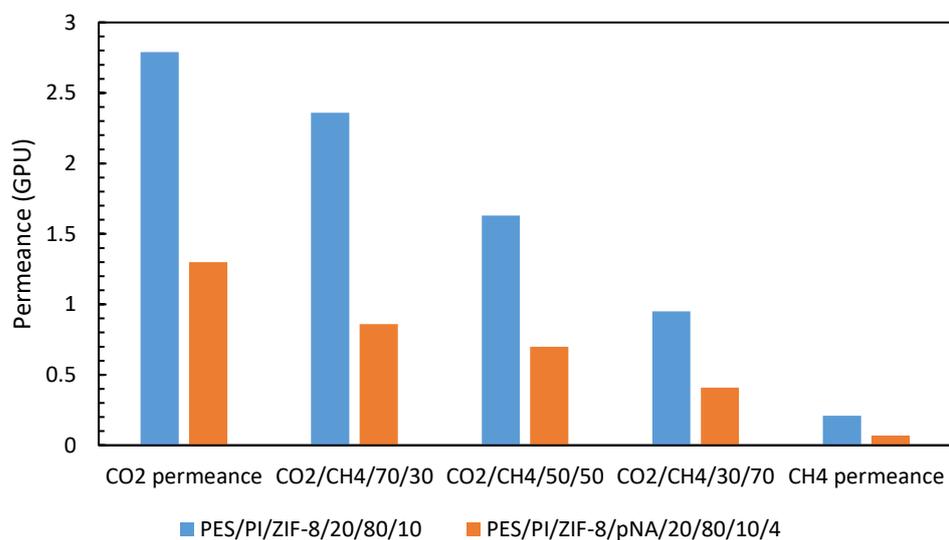
Figure 4.22 Compatibilizer (pNA) effect on permeances of PES/PI/ZIF-8/20/80/10 mixed matrix and PES/PI/ZIF-8/pNA/20/80/10/4 membranes (IR time: 40 sec.)

The membranes, which were given in Figure 4.22, were produced by using 40 sec. IR time and they were compared based on their permeances at 35 °C. In Figure 4.22, it was seen that the permeances substantially decreased for all of the feed gas compositions after the addition of pNA to the mixed matrix membrane.

Moreover, the effect of pNA on mixed matrix membrane selectivity was investigated. Therefore, the CO_2/CH_4 selectivity of PES/PI/ZIF-8/20/80/10 mixed matrix and PES/PI/ZIF-8/pNA/20/80/10/4 membranes were compared in Figure 4.23.
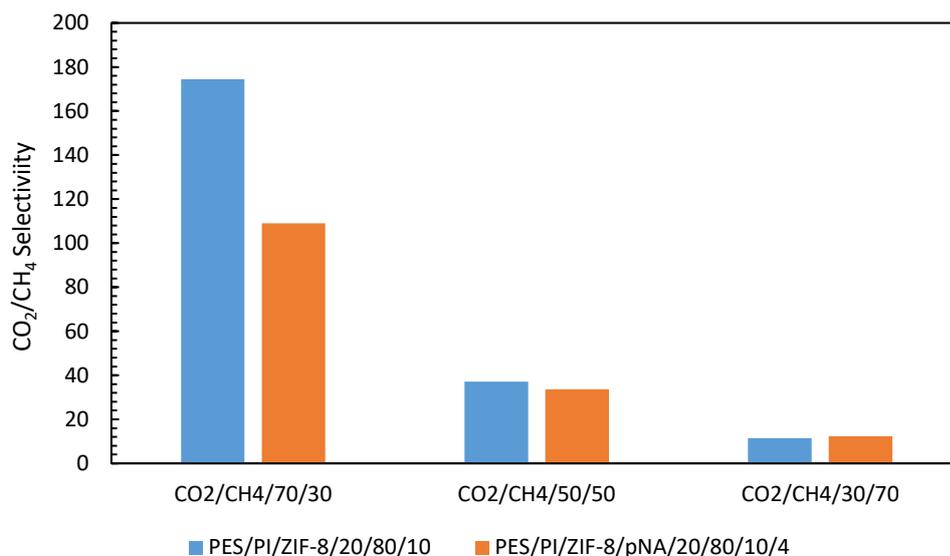
Figure 4.23 Compatibilizer (pNA) effect on CO_2/CH_4 selectivities of PES/PI/ZIF-8/20/80/10 mixed matrix and PES/PI/ZIF-8/pNA/20/80/10/4 membranes (IR time: 40 sec.)

According to Figure 4.23, the CO_2/CH_4 selectivity values of mixed matrix membrane decreased by adding pNA to the membrane at $CO_2/CH_4/70/30$ and $CO_2/CH_4/50/50$ feed gas compositions. On the other hand, when pNA addition caused a slight increase in the selectivity of $CO_2/CH_4/30/70$ feed.

4.5   Mixed Gas Separation Results for the Produced Membranes by using Liquid Water during Phase Inversion

In this study, the mixed gas separation measurements of the produced membranes by using liquid water during phase inversion were also carried out. Then, their permeance and selectivity analysis were performed based on temperature change and different feed gas compositions. The measured membranes were given in Table 4.13.

Table 4.13 The composition of the membranes produced by liquid water for mixed gas separation tests

Membrane Code	Membrane Name	PI wt.%	ZIF-8 wt.%
M7	PI36-P1	100	-
M8	M-PI1-P1	100	3

The permeance and selectivity trends of M7 and M8 membranes were investigated. The permeance versus temperature graph of M7 membrane were given in Figure 4.24.
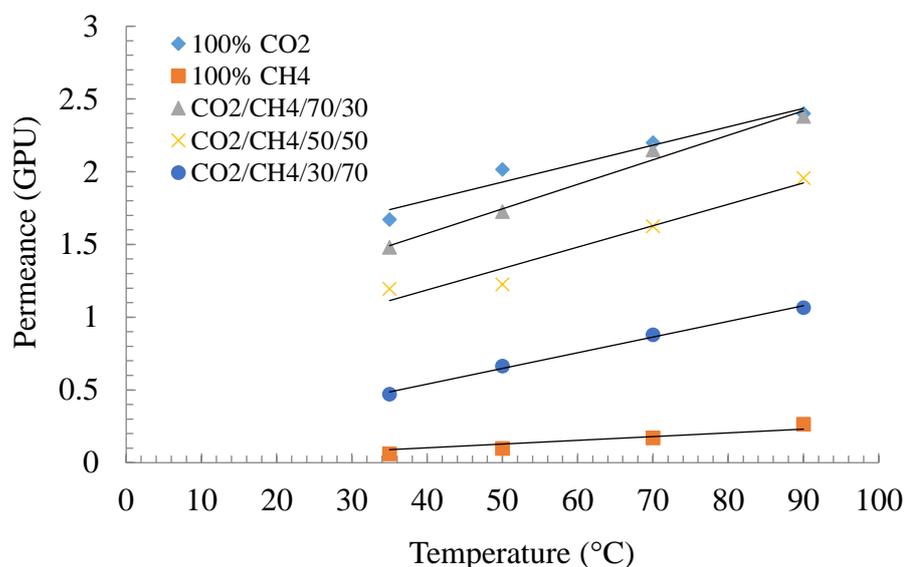
Figure 4.24 Permeance versus temprature graph of M7 membrane with different feed gas compositions

According to Figure 4.24, permeance values increased with increasing temperature. Moreover, it decreased with increasing the amount of CH_4 in feed gas composition. While the CO_2 permeances are in the range of 1.67 – 2.40 GPU, CH_4 permeances are in the range of 0.06 – 0.27 GPU. The other permeance values were placed between CO_2 and CH_4 permeance values. The permeance trends are

very similar with the trends of membranes which are produced by using water vapor induced phase inversion.

The CO_2/CH_4 selectivity versus temperature graph of M7 membrane was shown in Figure 4.25.
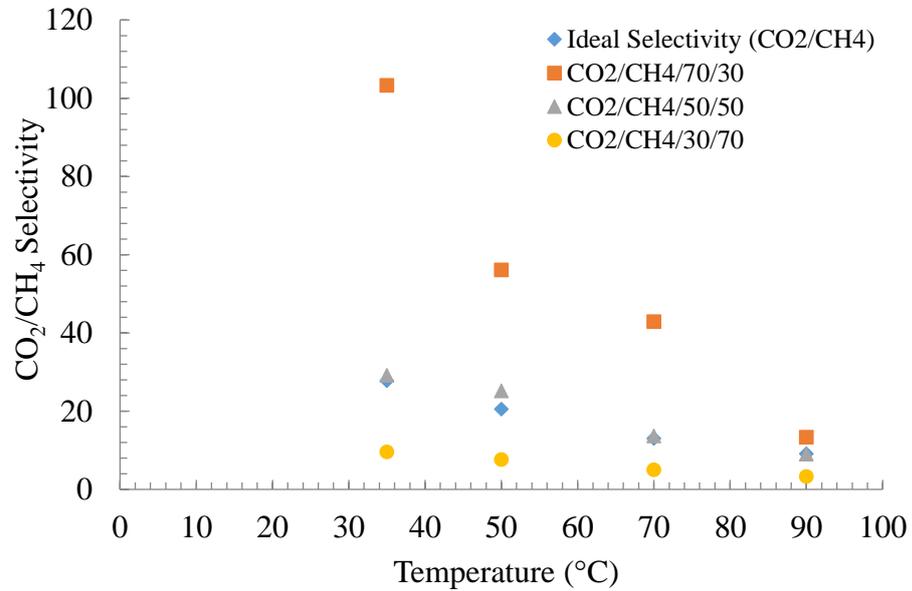
Figure 4.25 CO_2/CH_4 selectivity versus temperature graph of M7 membrane with different feed gas compositions

Because of the permeance values increased due to temperature rise, the CO_2/CH_4 selectivity values decreased. The highest selectivity value was obtained as 103.29 at 35°C and $CO_2/CH_4/70/30$ feed gas composition. On the other hand, the lowest value was 3.24 at 90°C and $CO_2/CH_4/30/70$ feed gas composition. Ideal selectivity values were calculated as very close to the values at $CO_2/CH_4/50/50$ feed gas compositions.

$CO_2\%$ in permeate vs. temperature and $CH_4\%$ in permeate vs. temperature graphs of M7 membrane at different feed gas compositions were represented in Figure 4.26 and Figure 4.27.
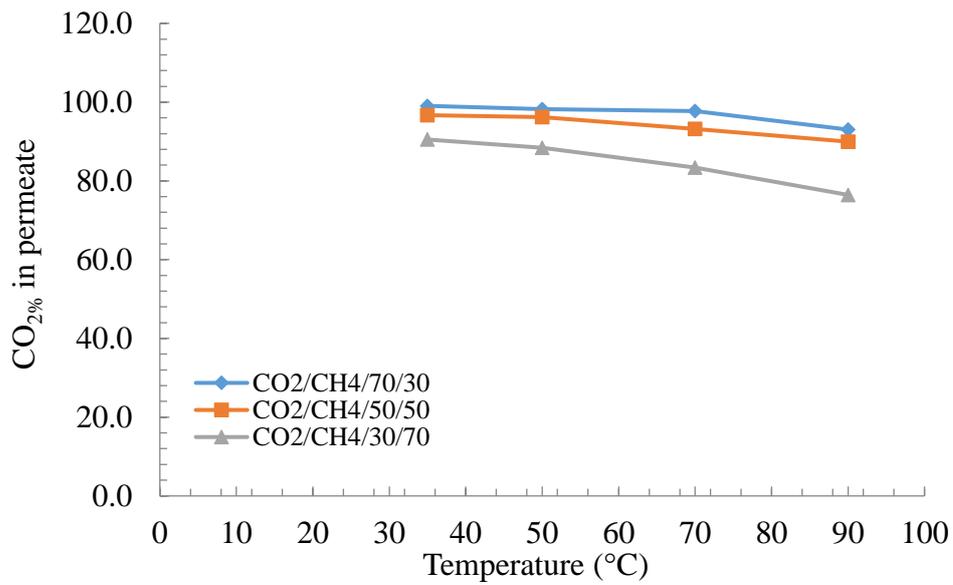
Figure 4.26 CO_2% in the permeate vs. temperature graph of M7 membrane for different feed gas compositions
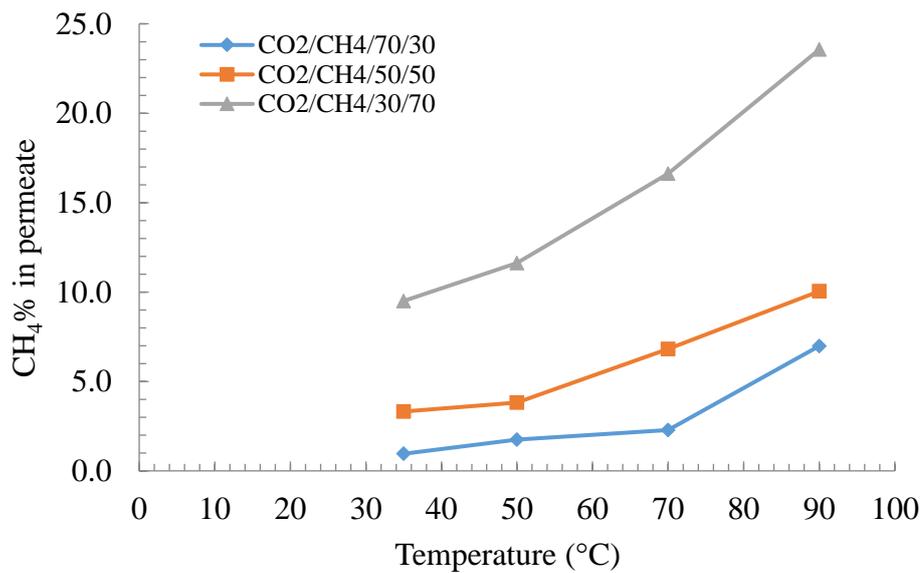
Figure 4.27 CH_4% in the permeate vs temerature graph of M7 membrane for different feed gas compositions

After the analysis of M7 membrane, the same examination was performed for the M8 membrane. The permeance versus temperature graph of M8 membrane were given in Figure 4.28.
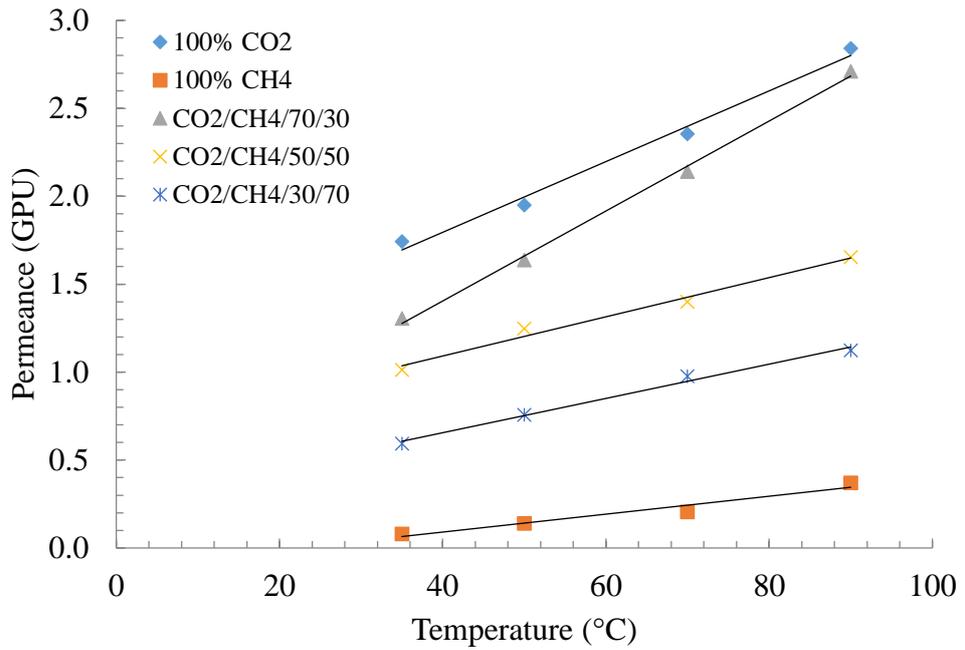
Figure 4.28 Permeance versus temprature graph of M8 membrane with different feed gas compositions

According to Figure 4.28, when the temperature increased, permeances of the M8 membrane also increased like M7 membrane. In addition, the amount of CH4 in the feed gas composition has the same effect on permeance values. While the CO_2 permeances increased from 1.74 to 2.84 GPU, CH_4 permeances increased from 0.08 to 0.37 GPU. The other permeance values at mixed CO_2/CH_4 feed gas compositions were placed between CO_2 and CH_4 permeance values.

The CO_2/CH_4 selectivity versus temperature graph of M8 membrane was given in Figure 4.29.
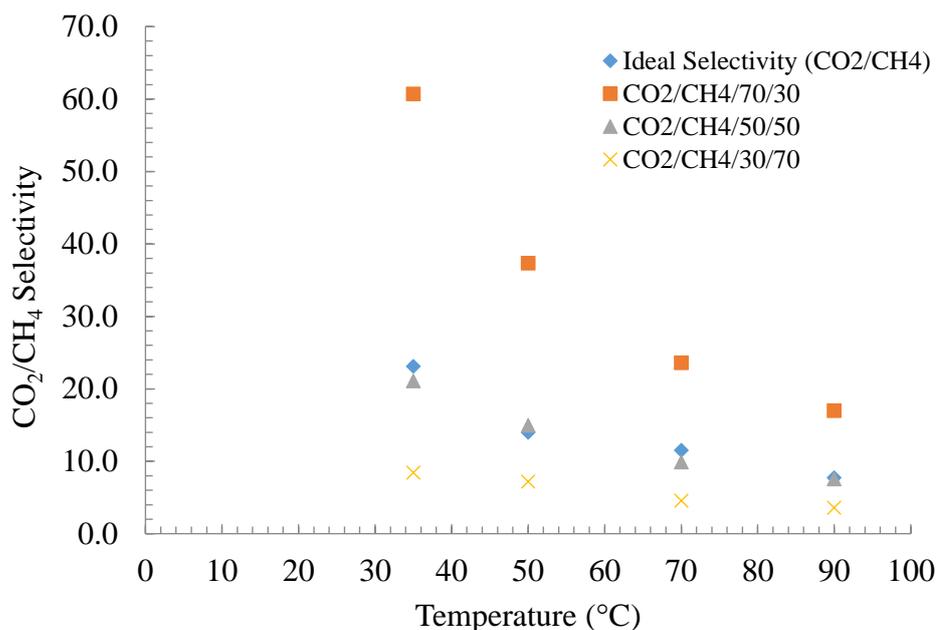
Figure 4.29 CO_2/CH_4 selectivity versus temperature graph of M8 membrane with different feed gas compositions

According to Figure 4.29, the CO_2/CH_4 selectivity values decreased with incresing temperature like M7 membrane. While the highest selectivity value was obtained as 60.72 at 35°C and $CO_2/CH_4/70/30$ feed gas composition, the lowest value was 3.57 at 90°C and $CO_2/CH_4/30/70$ feed gas composition. Ideal selectivity values were calculated as very close to the values at $CO_2/CH_4/50/50$ feed gas compositions again.

When the permeance and selectivity results of M7 and M8 membranes were compared, it can be said that filler material (ZIF-8) addition cause to increase permeances and decrease the CO_2/CH_4 selectivity values.

$CO_2\%$ in permeate vs. temperature and $CH_4\%$ in permeate vs. temperature graphs of M8 membrane at different feed gas compositions were represented in Figure 4.30 and Figure 4.31.
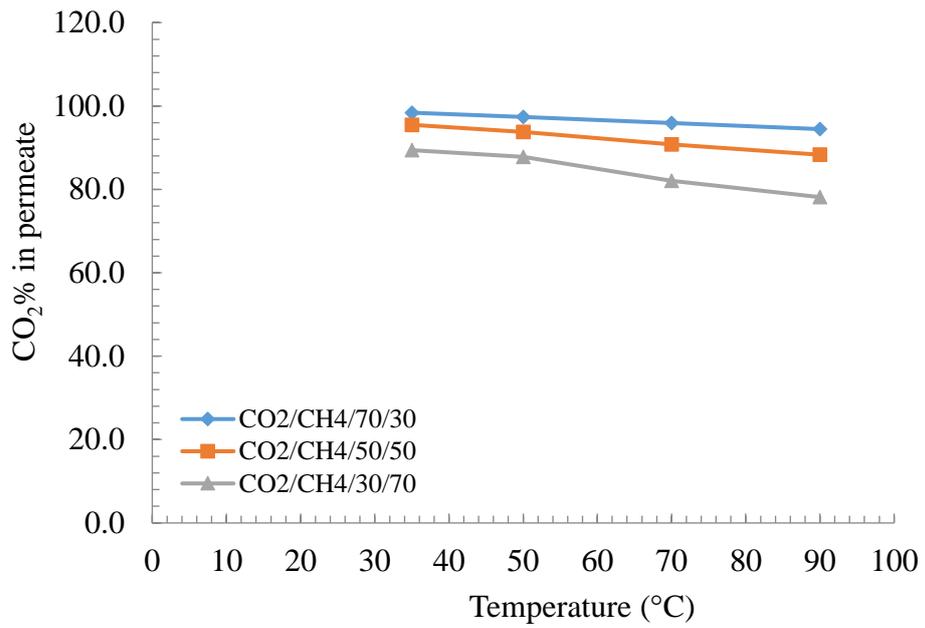
Figure 4.30 CO_2% in the permeate vs. temperature graph of M8 membrane for different feed gas compositions
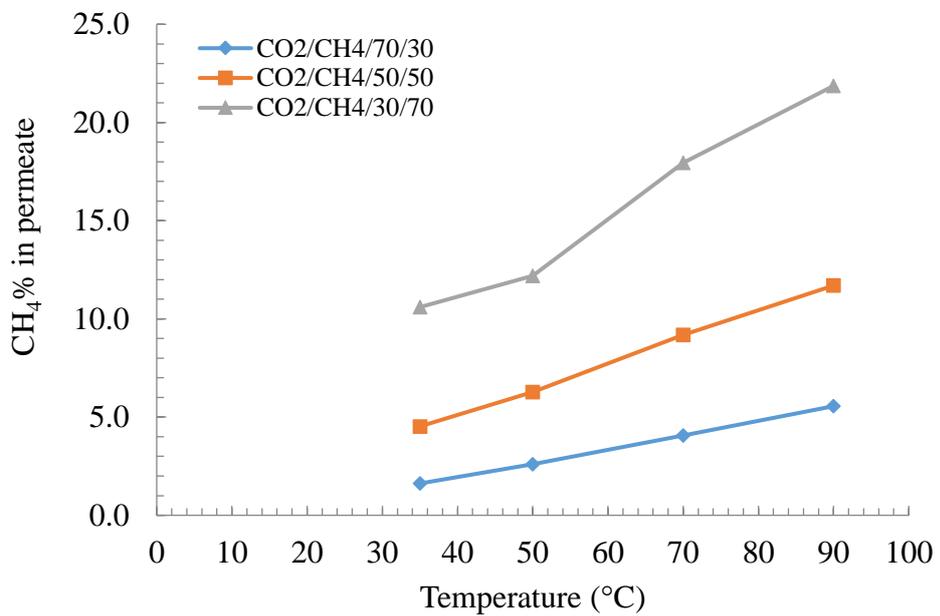
Figure 4.31 CH_4% in the permeate vs temerature graph of M8 membrane for different feed gas compositions

67

CHAPTER 5

CONCLUSIONS

In this study, single gas permeations of asymmetric PES/PI blend membranes and mixed matrix membranes with 10% ZIF-8 were tested at constant temperature and pressure. The wet phase inversion of membranes was performed by using water vapor at 80 % humidity while the dry phase inversion was made by infrared light. The casting process of membranes was carried out in the air conditining glove box to obtain desired ambient conditions. The polymers and ZIF-8 crystals used for membrane production were characterized by thermal gravimetric analysis (TGA), scanning electron microscopy (SEM), differential scanning calorimetry (DSC) and X-ray diffraction (XRD). The morphology of the produced membranes were determined by Scanning Electron Microscopy (SEM). H_2, CO_2 ve CH_4 gases were used for the gas permeation measurements through the membranes and ideal selectivity values of H_2/CO_2, CO_2/CH_4 ve H_2/CH_4 mixtures were calculated. The results obtained from the studies are given below:

1. XRD analysis was used to determine whether the desired crystallinity of produced ZIF-8 particles was achieved or not. As a results of analysis, it was observed that the values of ZIF-8 particles are the same with reference values. This result showed that produced ZIF-8 particles have the desired crystallinity.

2. TGA analysis was performed to determine the thermal behavior of produced polymers. As a results of this analysis, it was seen that the large proportion of weight loss of the blend membrane occurs above 450 °C. It was determined that weight loss increases as the amount of PI in the membrane decreases. It was also observed that the value of the decomposition temperature increses as the amount of PES in the same membranes increases. TGA analysis gives the results that the large proportion of weight loss of the mixed matrix membrane occurs above 400 °C and as the amount of ZIF-8 in the membranes increases weight loss of these membranes increases while decomposition temperatures decreases.

3. As a result of DSC analysis, it was observed that there is a decrease in the glass transition temperature of the blend membranes as the amount of PI in these membranes decreases. DSC analysis showed that the glass transition temperature decreases as the amount of ZIF-8 of theses membranes increases. No effect of the addition of compatibilizer PNA on the glass transition temperature was observed.

4. Based on the SEM images of the blend and mixed matrix membranes, pore structures of the membranes were found to be spongy structure. When the cross-sectional area of the mixed matrix membranes was considered, it was observed that the uniform distribution of ZIF-8 crystals along the cross section was not achieved and ZIF-8 crystals were clustered in the membrane pores.

5. According to the results of single gas permeation tests of the produced membranes, it was found that high ideal selectivity values of the membranes can be obtained but there are some problems about reproducibility of the membranes. The separation performance of the CO_2/CH_4 gas mixture of asymmetric blend and mixed matrix membranes was studied. Permeate was analyzed by using gas chromatography and CO_2/CH_4 selectivities were calculated. CO_2 and CH_4 permeabilities of the membranes were tested and CO_2/CH_4 ideal selectivities were calculated. As a results of analyses, the following results were obtained:

6. Based on the SEM images of the membranes, it was observed that the finger-like pore structure was obtained since the wet phase inversion of M-PI1-P1 (M2) membrane was carried out by using pure water. Pore structures of PES/PI/ZIF8/20/80/10 ve PES/PI/ZIF8/PNA/20/80/10/4 were found to be spongy structure because the wet phase inversion of these membranse was performed by using water vapor at 80 % humidity.

7. In the 4 membranes tested for mixed gas separation, permeability values were observed to increase with increasing temperature. Decrease in the amount of CO_2 in the feed gas decreased the CO_2/CH_4 selectivity of the membrane. As the temperature increased in gas permeability, the CO_2 / CH_4 ideal selectivity decreased. Although the production conditions of the tested 4 membranes are different from each other, the behavior related with the mixed gas separation performance of these membranes were the same.

REFERENCES

[1] Adewole, J., Ahmad, A., Ismail, S., & Leo, C. (2013). Current challenges in membrane separation of CO2 from natural gas: A review. *International Journal of Greenhouse Gas Control*, *17*, 46-65. doi:10.1016/j.ijggc.2013.04.012

[2] Seadi, T. A., Rutz, D., Prassl, H., Köttner, M., Finsterwalder, T., Volk, S., & Janssen, R. (2008). Biogas handbook. Retrieved from http://www.lemvigbiogas.com/BiogasHandbook.pdf

[3] Quintino, E. F., & Stock, J. A. (2014). A study about CO2/CH4 separation using polymeric membranes

[4] Baker, R. W. (2004). *Membrane technology and applications* (2nd ed.). Chichester: J. Wiley.

[5] Nasir, R., Mukhtar, H., Man, Z., & Mohshim, D. F. (2013). Material Advancements in Fabrication of Mixed-Matrix Membranes. *Chemical Engineering & Technology*, *36*(5), 717-727. doi:10.1002/ceat.201200734

[6] Kentish, S. E., Scholes, C. A., & Stevens, G. W. (2010). Carbon Dioxide Separation through Polymeric Membrane Systems for Flue Gas Applications. *Recent Patents on Chemical Engineering*, *1*(1), 52-66. doi:10.2174/1874478810801010052

[7] Kapantaidakis, G., & Koops, G. (2002). High flux polyethersulfone–polyimide blend hollow fiber membranes for gas separation. *Journal of Membrane Science*, *204*(1-2), 153-171. doi:10.1016/s0376-7388(02)00030-3

[8] Freeman, B. D. (1999). Basis of Permeability/Selectivity Tradeoff Relations in Polymeric Gas Separation Membranes. *Macromolecules*, *32*(2), 375-380. doi:10.1021/ma9814548

[9] Sanders D. F., Smith Z. P., Guo R., Robeson L. M., McGrath J. E., Paul D. R., Freeman B. D. (2013). Energy-efficient polymeric gas separation membranes for a sustainable future: A review, Polymer, 54 (2013), 4729-4761

71

[10] Sadrzadeh, M., & Bhattacharjee, S. (2013). Rational design of phase inversion membranes by tailoring thermodynamics and kinetics of casting solution using polymer additives. Journal of Membrane Science, 441, 31-44. doi:10.1016/j.memsci.2013.04.009

[11] Chae Park, H., Po Kim, Y., Yong Kim, H., & Soo Kang, Y. (1999). Membrane formation by water vapor induced phase inversion. *Journal of Membrane Science*, *156*(2), 169-178. doi:10.1016/s0376-7388(98)00359-7

[12] Blanco, J., Sublet, J., Nguyen, Q. T., & Schaetzel, P. (2006). Formation and morphology studies of different polysulfones-based membranes made by wet phase inversion process. *Journal of Membrane Science*, *283*(1-2), 27-37. doi:10.1016/j.memsci.2006.06.011

[13] Bushell, AF, Attfield, MP, Mason, CR, Budd, PM; Yampolskii, Y, Starannikova, L, Rebrov, A; Bazzarelli, F, Bernardo, P, Jansen, JC, Lanc, M, Friess, K, Shantarovich, V, Gustov, V, Isaeva, V.,"Gas permeation parameters of mixed matrix membranes based on the polymer of intrinsic microporosity PIM-1 and the zeolitic imidazolate framework ZIF-8", *Journal Of Membrane Science*, 427, 48-62, 2013.

[14] Zhang, Y., Musselman, I. H., Ferraris, J. P., & Balkus, K. J. (2008). Gas permeability properties of Matrimid® membranes containing the metal-organic framework Cu–BPY–HFS. *Journal of Membrane Science*, *313*(1-2), 170-181. doi:10.1016/j.memsci.2008.01.005

[15] Phan, A., Doonan, C. J., Uribe-Romo, F. J., Knobler, C. B., O'Keeffe, M., & Yaghi, O. M. (2010). Synthesis, Structure, and Carbon Dioxide Capture Properties of Zeolitic Imidazolate Frameworks. *Accounts of Chemical Research*, *43*(1), 58-67. doi:10.1021/ar900116g

[16] Cacho-Bailo, F., Seoane, B., Téllez, C., & Coronas, J. (2014). ZIF-8 continuous membrane on porous polysulfone for hydrogen separation. *Journal of Membrane Science*, *464*, 119-126. doi:10.1016/j.memsci.2014.03.070

[17] J. Han, W. Lee, J.M. Choi, R. Patel, B.R. Min, Characterization of polyethersulfone/polyimide blend membranes prepared by a dry/wet phase inversion: Precipitation kinetics, morphology and gas separation, J. Memb. Sci. 351 (2010) 141–148. doi:10.1016/j.memsci.2010.01.038

[18] S. Rafiq, Z. Man, A. Maulud, N. Muhammad, S. Maitra, Effect of varying solvents compositions on morphology and gas permeation properties on

membranes blends for CO2 separation from natural gas, J. Memb. Sci. 378 (2011) 444–452. doi:10.1016/j.memsci.2011.05.025.

[19] S. Basu, A. Cano-Odena, I.F.J. Vankelecom, Asymmetric membrane based on Matrimid® and polysulphone blends for enhanced permeance and stability in binary gas (CO2/CH4) mixture separations, Sep. Purif. Technol. 75 (2010) 15–21. doi:10.1016/j.seppur.2010.07.004

[20] G.C. Kapantaidakis, G.H. Koops, High flux polyethersulfone–polyimide blend hollow fiber membranes for gas separation, J. Memb. Sci. 204 (2002) 153–171. doi:10.1016/S0376-7388(02)00030-3.

[21] S.S. Hosseini, N. Peng, T.S. Chung, Gas separation membranes developed through integration of polymer blending and dual-layer hollow fiber spinning process for hydrogen and natural gas enrichments, J. Memb. Sci. 349 (2010) 156–166. doi:10.1016/j.memsci.2009.11.043

[22] S. Basu, A. Cano-Odena, I.F.J. Vankelecom, Asymmetric Matrimid®/[Cu3(BTC)2] mixed-matrix membranes for gas separations, J. Memb. Sci. 362 (2010) 478–487. doi:10.1016/j.memsci.2010.07.005

[23] S. Rafiq, Z. Man, A. Maulud, N. Muhammad, S. Maitra, Separation of CO2 from CH4 using polysulfone/polyimide silica nanocomposite membranes, Sep. Purif. Technol. 90 (2012) 162–172. doi:10.1016/j.seppur.2012.02.031.

[24] Guan, R., Zou, H., Lu, D., Gong, C., & Liu, Y. (2005). Polyethersulfone sulfonated by chlorosulfonic acid and its membrane characteristics. *European Polymer Journal*, *41*(7), 1554-1560. doi:10.1016/j.eurpolymj.2005.01.018

[25] Han, J., Lee, W., Choi, J. M., Patel, R., & Min, B. (2010). Characterization of polyethersulfone/polyimide blend membranes prepared by a dry/wet phase inversion: Precipitation kinetics, morphology and gas separation. *Journal of Membrane Science*, *351*(1-2), 141-148. doi:10.1016/j.memsci.2010.01.038

[26] N. Keser Demir, B. Topuz, L. Yilmaz, H. Kalipcilar, Synthesis of ZIF-8 from recycled mother liquors, Microporous Mesoporous Mater. 198 (2014) 291–300. doi:10.1016/j.micromeso.2014.07.052.

[27] N. Keser, Production and Performance Evaluation of ZIF-8 Based Binary and Ternary Mixed Matrix Gas Separation Membranes, Middle East Technical University, 2012

APPENDICES

A. SINGLE GAS PERMEANCE CALCULATION

In order to calculate single gas permeance of a membrane, dependency of pressure change in permeate with respect to time is investigated. During the gas permeation experiment, the data related with pressure change are recorded by using a computer program. A sample pressure change with respect to time is represented in Figure dfgdfg and sample calculations for single gas permeance are given.
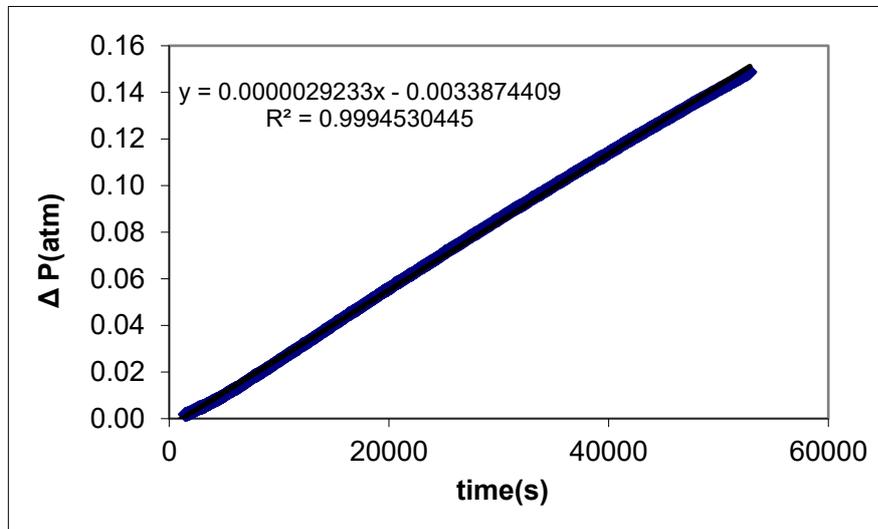
Figure A.1 CO_2 permeance test at 35°C for PES/PI/20/80

ΔP is calculated by subtraction of the initial pressure from n^{th} pressure, that is

$$\Delta P = P_n - P_0 \qquad (A.1)$$

The slope of the graph gives ΔP/Δt value and then, the rate of change of moles can be calculated.

$$\frac{\Delta n}{\Delta t} = \left[\frac{\Delta P}{\Delta t} \times V_d\right] / RT \qquad (A.2)$$

where

V_d: dead volume of the permeate side

Volumetric rate of change is

$$\frac{\Delta V}{\Delta t} = \left[\frac{\Delta n}{\Delta t} \times MW\right] / \rho \qquad (A.3)$$

where

MW: molecular weight of the gas

ρ: density of the gas

Volumetric flow rate per effective membrane area (A) gives the gas flux (J) through the membrane.

$$J = \frac{\Delta V / \Delta t}{A} \qquad (A.4)$$

Finally, gas permeability of the membrane is calculated by using following equation:

$$P = \frac{J \times l}{P_f - P_p} \qquad (A.5)$$

where

l: membrane thickness

Pf: Feed pressure

Pp: Permeate pressure

B. SINGLE GAS PERMEATION RESULTS FOR BLEND AND MIXED MATRIX MEMBRANES

The single gas permeance and ideal selectivities of all blend and mixed matrix membranes produced with different IR time were tabulated in Table B.1. While the numbers used in membrane name represents which membrane produced, the used latters represents which pieces of the same membrane. For example, "1" states that the membrane is the first produced membranes and "a" states that first pieces of the first produced membrane for the membrane named as PES/PI/20/80-1a. The H_2, CO_2 and CH_4 permeance and ideal selectivities of all of the membranes produced by different IR time during the dry phase inversion were given below.

Table B.1 H_2, CO_2, CH_4 permeance and ideal selectivities of blend and mixed matrix membranes

Membrane Type	Permeance (GPU)			Ideal Selectivity		
	H_2	CO_2	CH_4	H_2/CO_2	CO_2/CH_4	H_2/CH_4
PES/PI/20/80-4a (IR: 0 sec.)	4.22	1.57	0.06	2.7	26.2	70.3
PES/PI/20/80-6a (IR: 0 sec.)	6.05	2.32	0.09	2.6	25.8	67.2
PES/PI/20/80-8a (IR: 0 sec.)	6.00	1.70	0.06	3.5	28.3	100.0
PES/PI/20/80-1a (IR: 40 sec.)	5.88	5.40	0.11	1.1	49.1	53.5
PES/PI/20/80-2a (IR: 40 sec.)	4.40	2.28	0.09	1.9	25.3	48.9
PES/PI/20/80-5a (IR: 80 sec.)	3.31	1.21	0.05	2.7	24.2	66.2
PES/PI/20/80-7a (IR: 80 sec.)	3.34	1.24	0.05	2.7	24.8	66.8
PES/PI/20/80-9a (IR: 80 sec.)	3.21	1.16	0.05	2.8	23.2	64.2
PES/PI/20/80-3a (IR: 120 sec.)	0.55	0.38	0.02	1.5	19.7	28.9
PES/PI/50/50-1a (IR: 40 sec.)	5.50	3.00	0.13	1.8	23.1	42.3
PES/PI/50/50-2a (IR: 120 sec.)	1.74	0.90	0.09	1.9	10.0	19.3
PES/PI/80/20-3a (IR: 120 sec.)	5.37	2.08	0.09	2.6	23.1	59.7
PES/PI/ZIF-8/20/80/10-9a (IR: 0 sec.)	14.22	5.26	0.40	2.7	13.2	35.6
PES/PI/ZIF-8/20/80/10-2a (IR: 40 sec.)	3.25	2.12	0.08	1.5	26.2	40.6
PES/PI/ZIF-8/20/80/10-10a (IR: 40 sec.)	6.30	2.52	0.09	2.5	28.0	70.0
PES/PI/ZIF-8/20/80/10-7a (IR: 80 sec.)	5.58	2.05	0.09	2.7	23.8	64.9
PES/PI/ZIF-8/20/80/10-7a (IR: 80 sec.)	4.71	1.74	0.07	2.7	24.9	67.3
PES/PI/ZIF-8/20/80/10-8a (IR: 120 sec.)	1.81	0.77	0.03	2.4	25.7	60.3
PES/PI/ZIF-8/20/80/10-12a (IR: 120 sec.)	1.84	0.80	0.04	2.3	20.0	46.0
PES/PI/ZIF-8/50/50/10-1a (IR: 40 sec.)	9.99	5.16	0.77	1.9	6.7	13.0
PES/PI/ZIF-8/80/20/10-2a (IR: 40 sec.)	5.18	2.05	0.07	2.5	29.3	74.0

C. MIXED GAS SEPARATION RESULTS FOR BLEND AND MIXED MATRIX MEMBRANES

The CO_2 and CH_4 gas permeance and CO_2/CH_4 selectivity values of the produced blend and mixed matrix membranes which are coded as M1, M2, M3, M4, M5 and M6 in Results and Discussion part were tabulated below.

For M1 membrane, the CO_2 and CH_4 gas permeance and CO_2/CH_4 selectivity values were given in Table C.1 and Table C.2.

Table C.1 CO_2 and CH_4 permeances and ideal selectivities of M1 membrane at different temperatures

Temperature (°C)	Pure CO_2 Permeance (GPU)	Pure CH_4 Permeance (GPU)	Ideal Selectivity
35	1.17	0.05	23.33
50	1.64	0.09	18.99
70	2.06	0.16	12.70
90	2.42	0.29	8.38

Table C.2 CO_2 and CH_4 permeances, CO_2/CH_4 selectivities and permeate compositions of M1 membrane at different temperatures

Temperature (°C)	$CO_2/CH_4/70/30$ Permeance (GPU)	CO_2/CH_4 Selectivity	$CO_2\%$ in the permeate	$CH_4\%$ in the permeate
35	1.11	146.93	99.324	0.676
50	1.42	76.30	98.706	1.294
70	1.76	39.70	97.543	2.457
90	2.16	36.50	97.333	2.667
Temperature (°C)	$CO_2/CH_4/50/50$ Permeance (GPU)	CO_2/CH_4 Selectivity	$CO_2\%$ in the permeate	$CH_4\%$ in the permeate
35	0.87	84.84	98.835	1.165
50	1.08	40.25	97.576	2.424
70	1.33	19.21	95.051	4.949
90	1.68	11.70	92.124	7.876
Temperature (°C)	$CO_2/CH_4/30/70$ Permeance (GPU)	CO_2/CH_4 Selectivity	$CO_2\%$ in the permeate	$CH_4\%$ in the permeate
35	0.64	35.40	97.253	2.747
50	0.82	17.83	94.689	5.311
70	1.03	7.83	88.679	11.321
90	1.26	5.27	84.046	15.594

For M2 membrane, the CO_2 and CH_4 gas permeance and CO_2/CH_4 selectivity values were given in Table C.3 and Table C.4.

Table C.3 CO_2 and CH_4 permeances and ideal selectivities of M2 membrane at different temperatures

Temperature (°C)	Pure CO_2 Permeance (GPU)	Pure CH_4 Permeance (GPU)	Ideal Selectivity
35	0.86	0.03	28.67
50	1.12	0.08	14.00
70	1.37	0.14	9.79
90	1.71	0.24	7.13

Table C.4 CO_2 and CH_4 permeances, CO_2/CH_4 selectivities and permeate compositions of M2 membrane at different temperatures

Temperature (°C)	$CO_2/CH_4/70/30$ Permeance (GPU)	CO_2/CH_4 Selectivity	$CO_2\%$ in the permeate	$CH_4\%$ in the permeate
35	0.63	153.06	99.351	0.649
50	0.87	68.63	98.564	1.436
70	1.16	38.70	97.481	2.519
90	1.50	23.77	95.963	4.037
Temperature (°C)	$CO_2/CH_4/50/50$ Permeance (GPU)	CO_2/CH_4 Selectivity	$CO_2\%$ in the permeate	$CH_4\%$ in the permeate
35	0.48	50.52	98.059	1.941
50	0.70	37.78	97.421	2.579
70	0.85	18.14	94.774	5.226
90	1.11	9.86	90.794	9.206
Temperature (°C)	$CO_2/CH_4/30/70$ Permeance (GPU)	CO_2/CH_4 Selectivity	$CO_2\%$ in the permeate	$CH_4\%$ in the permeate
35	0.35	28.50	96.611	3.389
50	0.46	12.05	92.338	7.662
70	0.65	7.23	87.849	12.151
90	0.87	4.57	82.039	17.961

For M3 membrane, the CO_2 and CH_4 gas permeance and CO_2/CH_4 selectivity values were given in Table C.5 and Table C.6.

Table C.5 CO_2 and CH_4 permeances and ideal selectivities of M3 membrane at different temperatures

Temperature (°C)	Pure CO_2 Permeance (GPU)	Pure CH_4 Permeance (GPU)	Ideal Selectivity
35	5.43	0.39	13.92
50	6.67	0.58	11.50
70	7.86	0.95	8.27
90	8.88	1.44	6.17

Table C.6 CO_2 and CH_4 permeances, CO_2/CH_4 selectivities and permeate compositions of M3 membrane at different temperatures

Temperature (°C)	$CO_2/CH_4/70/30$ Permeance (GPU)	CO_2/CH_4 Selectivity	$CO_2\%$ in the permeate	$CH_4\%$ in the permeate
35	3.61	41.46	97.645	2.355
50	4.40	24.92	96.142	3.858
70	5.14	13.35	93.029	6.971
90	6.53	10.65	91.415	8.585
Temperature (°C)	$CO_2/CH_4/50/50$ Permeance (GPU)	CO_2/CH_4 Selectivity	$CO_2\%$ in the permeate	$CH_4\%$ in the permeate
35	2.64	19.72	95.174	4.826
50	3.02	9.15	90.145	9.855
70	4.08	6.62	86.885	13.115
90	4.86	4.52	81.885	18.115
Temperature (°C)	$CO_2/CH_4/30/70$ Permeance (GPU)	CO_2/CH_4 Selectivity	$CO_2\%$ in the permeate	$CH_4\%$ in the permeate
35	1.73	8.79	89.790	10.210
50	2.05	5.79	85.263	14.737
70	2.62	2.72	73.134	26.866
90	3.47	2.03	67.039	32.961

For M4 membrane, the CO_2 and CH_4 gas permeance and CO_2/CH_4 selectivity values were given in Table C.7 and Table C.8.

Table C.7 CO_2 and CH_4 permeances and ideal selectivities of M4 membrane at different temperatures

Temperature (°C)	Pure CO_2 Permeance (GPU)	Pure CH_4 Permeance (GPU)	Ideal Selectivity
35	2.79	0.21	13.67
50	3.79	0.27	14.35
70	4.62	0.41	11.28
90	5.28	0.63	8.25

Table C.8 CO_2 and CH_4 permeances, CO_2/CH_4 selectivities and permeate compositions of M4 membrane at different temperatures

Temperature (°C)	$CO_2/CH_4/70/30$ Permeance (GPU)	CO_2/CH_4 Selectivity	$CO_2\%$ in the permeate	$CH_4\%$ in the permeate
35	2.36	174.46	99.430	0.570
50	3.19	58.51	98.320	1.680
70	3.78	32.53	97.018	2.982
90	4.86	25.65	96.248	3.752

Temperature (°C)	$CO_2/CH_4/50/50$ Permeance (GPU)	CO_2/CH_4 Selectivity	$CO_2\%$ in the permeate	$CH_4\%$ in the permeate
35	1.63	37.11	97.376	2.624
50	2.08	22.98	95.831	4.169
70	2.64	14.90	93.710	6.290
90	2.95	8.98	89.985	10.015

Temperature (°C)	$CO_2/CH_4/30/70$ Permeance (GPU)	CO_2/CH_4 Selectivity	$CO_2\%$ in the permeate	$CH_4\%$ in the permeate
35	0.95	11.39	91.931	8.069
50	1.20	8.09	88.995	11.005
70	1.55	5.27	84.049	15.951
90	1.80	4.15	80.577	19.423

For M5 membrane, the CO_2 and CH_4 gas permeance and CO_2/CH_4 selectivity values were given in Table C.9 and Table C.10.

Table C.9 CO_2 and CH_4 permeances and ideal selectivities of M5 membrane at different temperatures

Temperature (°C)	Pure CO_2 Permeance (GPU)	Pure CH_4 Permeance (GPU)	Ideal Selectivity
35	1.33	0.07	19.00
50	1.75	0.14	12.50
70	2.18	0.23	9.48
90	2.97	0.44	6.75

Table C.10 CO_2 and CH_4 permeances, CO_2/CH_4 selectivities and permeate compositions of M5 membrane at different temperatures

Temperature (°C)	$CO_2/CH_4/70/30$ Permeance (GPU)	CO_2/CH_4 Selectivity	$CO_2\%$ in the permeate	$CH_4\%$ in the permeate
35	1.26	98.85	98.999	1.001
50	1.58	56.00	98.246	1.754
70	1.93	35.61	97.268	2.732
90	2.36	22.60	95.762	4.238

Temperature (°C)	$CO_2/CH_4/50/50$ Permeance (GPU)	CO_2/CH_4 Selectivity	$CO_2\%$ in the permeate	$CH_4\%$ in the permeate
35	0.91	43.38	97.747	2.253
50	1.22	15.67	94.000	6.000
70	1.42	11.96	92.286	7.714
90	1.77	8.30	89.244	10.756

Temperature (°C)	$CO_2/CH_4/30/70$ Permeance (GPU)	CO_2/CH_4 Selectivity	$CO_2\%$ in the permeate	$CH_4\%$ in the permeate
35	0.57	17.84	94.692	5.308
50	0.70	7.71	88.518	11.482
70	1.02	6.59	86.826	13.174
90	1.25	4.18	80.695	19.305

For M6 membrane, the CO_2 and CH_4 gas permeance and CO_2/CH_4 selectivity values were given in Table C.11 and Table C.12.

Table C.11 CO_2 and CH_4 permeances and ideal selectivities of M6 membrane at different temperatures

Temperature (°C)	Pure CO_2 Permeance (GPU)	Pure CH_4 Permeance (GPU)	Ideal Selectivity
35	1.30	0.07	20.12
50	1.65	0.11	15.70
70	2.12	0.18	12.19
90	2.69	0.29	9.32

Table C.12 CO_2 and CH_4 permeances, CO_2/CH_4 selectivities and permeate compositions of M6 membrane at different temperatures

Temperature (°C)	$CO_2/CH_4/70/30$ Permeance (GPU)	CO_2/CH_4 Selectivity	$CO_2\%$ in the permeate	$CH_4\%$ in the permeate
35	0.86	109.02	99.091	0.909
50	1.19	53.64	98.170	1.830
70	1.68	34.41	97.176	2.824
90	2.23	20.12	95.264	4.736
Temperature (°C)	$CO_2/CH_4/50/50$ Permeance (GPU)	CO_2/CH_4 Selectivity	$CO_2\%$ in the permeate	$CH_4\%$ in the permeate
35	0.70	33.63	97.112	2.888
50	0.91	19.74	95.178	4.822
70	1.24	12.89	92.799	7.201
90	1.61	6.87	87.294	12.706
Temperature (°C)	$CO_2/CH_4/30/70$ Permeance (GPU)	CO_2/CH_4 Selectivity	$CO_2\%$ in the permeate	$CH_4\%$ in the permeate
35	0.41	12.28	92.470	7.530
50	0.55	8.75	89.744	10.256
70	0.73	4.84	82.887	17.113
90	1.00	3.70	78.713	21.287

D. MIXED GAS SEPARATION RESULTS FOR THE PRODUCED MEMBRANES BY USING LIQUID WATER DURING PHASE INVERSION

The CO_2 and CH_4 gas permeance and CO_2/CH_4 selectivity values of the membranes produced by using liquid water during phase inversion which are coded M7 and M8 in Results and Discussion part were given below.

For M7 membrane, the CO_2 and CH_4 gas permeance and CO_2/CH_4 selectivity values were given in

Table D.1 CO2 and CH4 permeances and ideal selectivities of M7 membrane at different temperatures

Temperature (°C)	Pure CO_2 Permeance (GPU)	Pure CH_4 Permeance (GPU)	Ideal Selectivity
35	1.67	0.06	27.77
50	2.02	0.10	20.50
70	2.20	0.17	12.97
90	2.40	0.27	9.08

E. CALIBRATION CURVES OF CO_2 AND CH_4 GASES FOR GAS CHROMATOGRAPHY
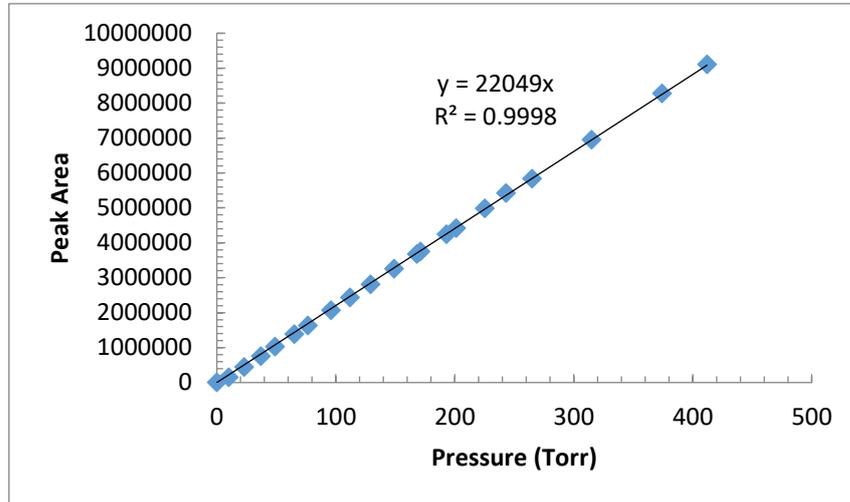
Figure E.1 Calibration curve for CO_2 gas
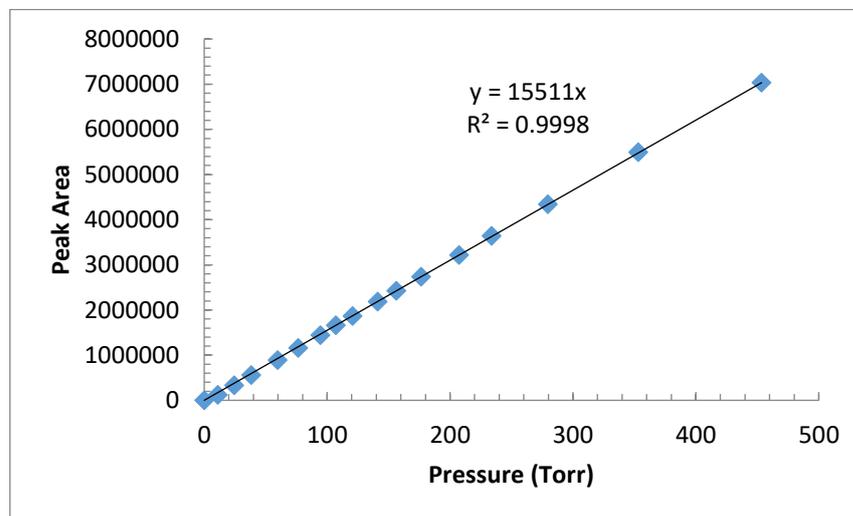
Figure E.2 Calibration curve of CH_4 gas

## F. TGA THERMOGRAMS OF ASYMMETRIC BLEND AND MIXED MATRIX MEMBRANES
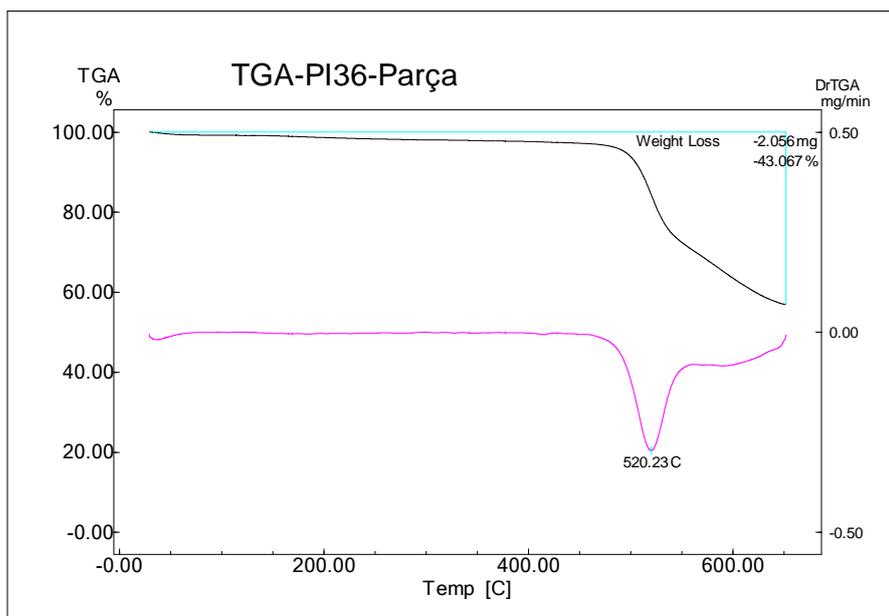
Figure F.1 Thermogram of pure PI (PI36)
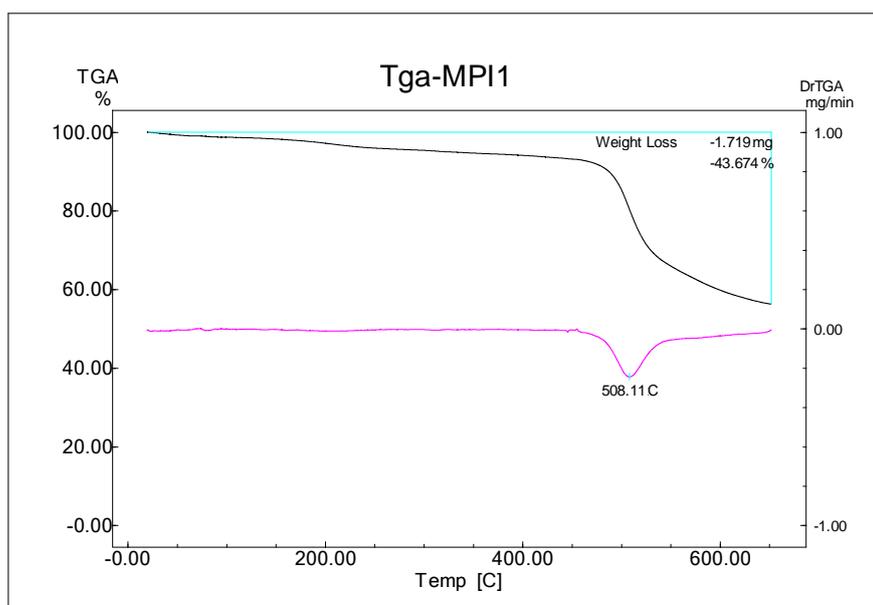

Figure F.2Thermogram of M-PI1-P1
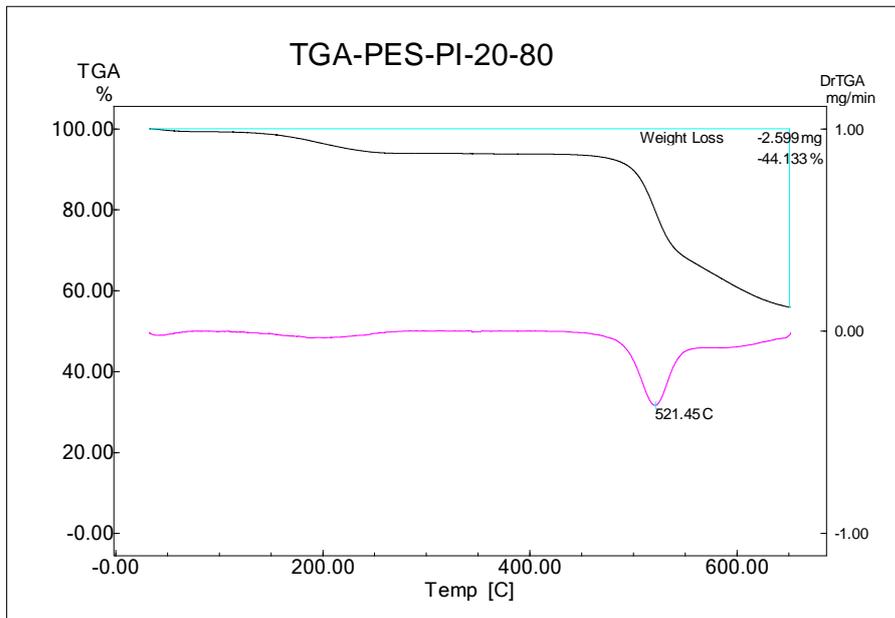
Figure F.3 Thermogram of PES/PI/20/80
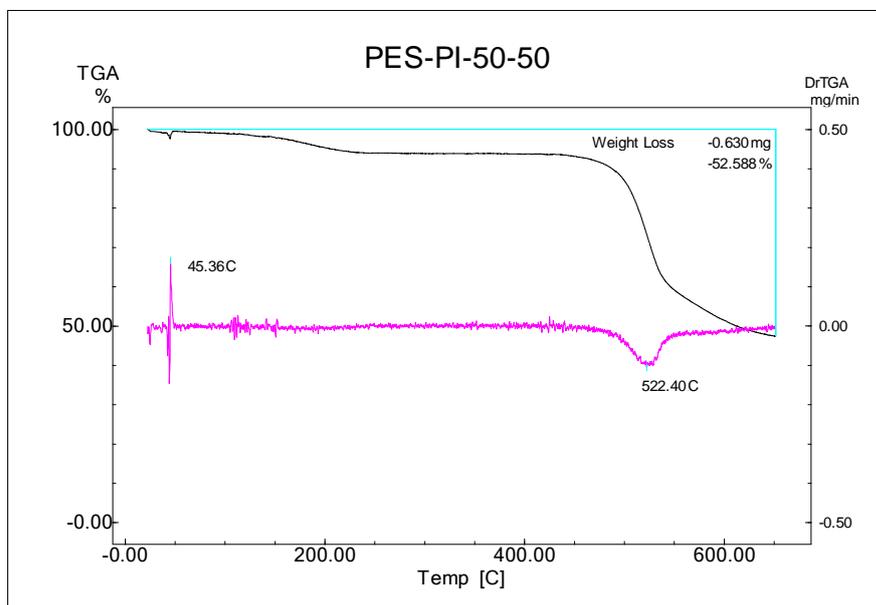

Figure F.4 Thermogram of PES/PI/50/50
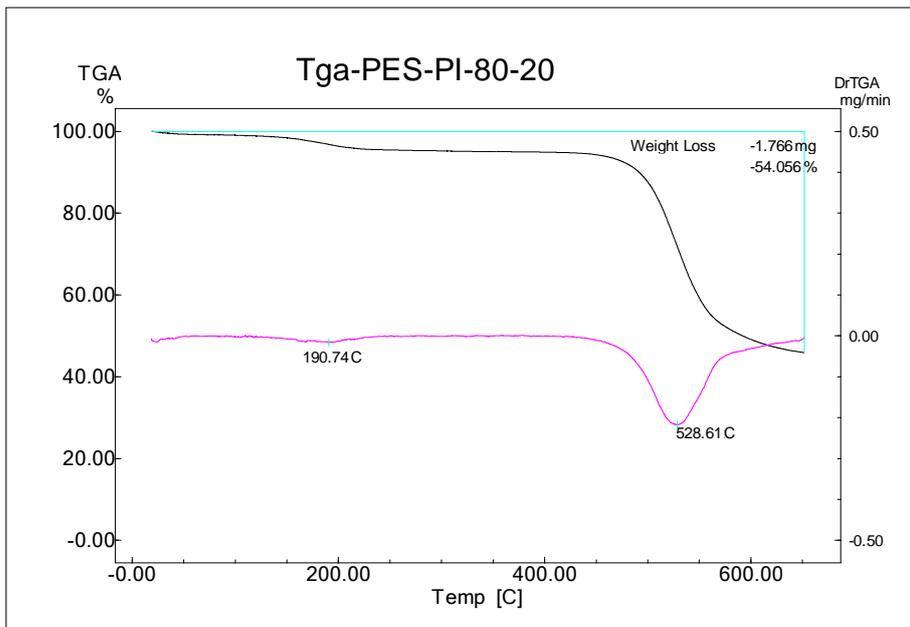
Figure F.5Thermogram of PES/PI/80/20
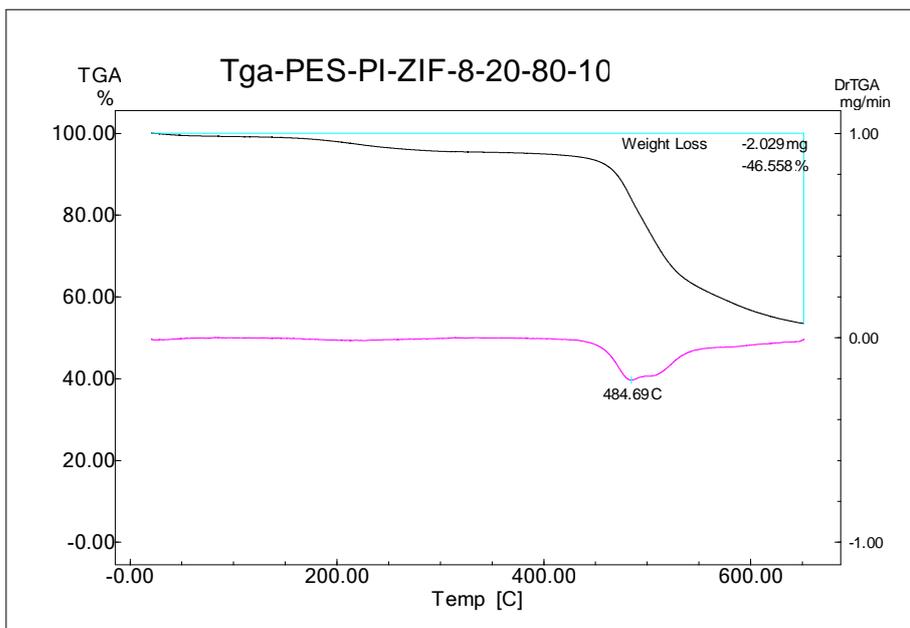
Figure F.6 Thermogram of PES/PI/ZIF-8/20/80/10
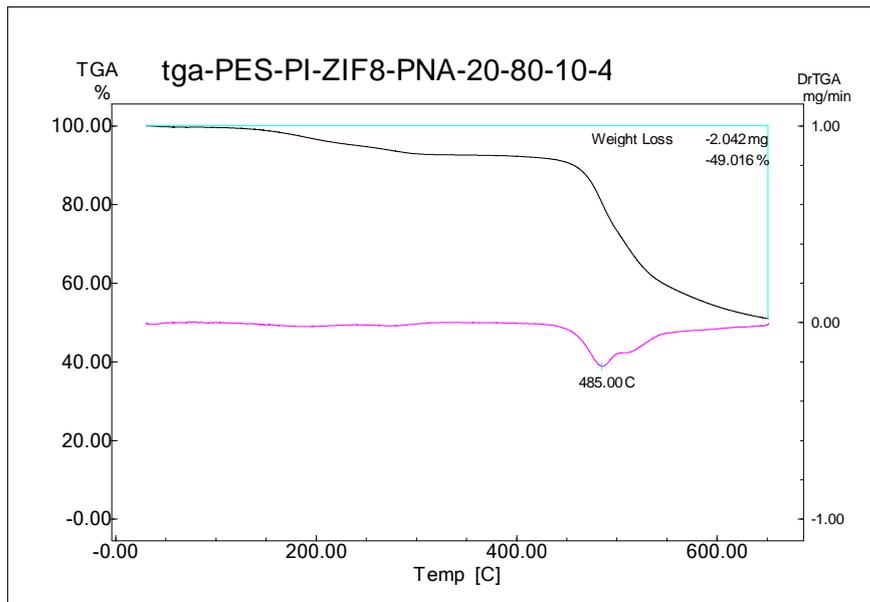
Figure F.7Thermogram of PES/PI/ZIF8/pNA/20/80/10/4